Published in final edited form as:

Mol Microbiol. 2013 April ; 88(1): 105–124. doi:10.1111/mmi.12171.

Borrelia host adaptation Regulator (BadR) regulates *rpoS* to modulate host adaptation and virulence factors in *Borrelia burgdorferi*

Christine L. Miller, **S. L. Rajasekhar Karna**, and **J. Seshu***

South Texas Center for Emerging Infectious Diseases, Center for Excellence in Infection Genomics and Department of Biology, The University of Texas at San Antonio

SUMMARY

The RpoS transcription factor of *Borrelia burgdorferi* is a "gatekeeper" because it activates genes required for spirochetes to transition from tick to vertebrate hosts. However, it remains unknown how RpoS becomes repressed to allow the spirochetes to transition back from the vertebrate host to the tick vector. Here we show that a putative carbohydrate-responsive regulatory protein, designated BadR (Borrelia host adaptation Regulator), is a transcriptional repressor of *rpoS*. BadR levels are elevated in *B. burgdorferi* cultures grown under *in vitro* conditions mimicking unfed-ticks and *badR*-deficient strains are defective for growth under these same conditions. Microarray and immunoblot analyses of *badR*-deficient strains showed up-regulation of *rpoS* and other factors important for virulence in vertebrate hosts, as well as down-regulation of putative tick-specific determinants (e.g. linear plasmid 28-4 genes). DNA-binding assays revealed BadR binds to upstream regions of *rpoS*. Site-directed mutations in BadR and the presence of phosphorylated sugars affected BadR's binding to the *rpoS* promoters. *badR*-deficient *B. burgdorferi* were unable to colonize mice. Several putative tick-specific targets have been identified. Our study identified a novel regulator, BadR, and provides a link between nutritional environmental cues utilized by spirochetes to adaptation to disparate conditions found in the tick and vertebrate hosts.

INTRODUCTION

Lyme disease is a persistent multi-system inflammatory disease and the most frequently reported arthropod-borne disease in the U.S. with over 30,000 cases reported to the Centers for Disease Control and Prevention (CDC) in 2010. Currently, there is no vaccine available and the CDC has classified Lyme disease as a re-emerging infection (CDC, 2012).

Borrelia burgdorferi, the etiologic agent of Lyme disease, is a spirochetal pathogen that exists in nature in an enzootic cycle between its tick and vertebrate hosts (Steere, 2006; Barbour *et al.*, 1983). The spirochetes' ability to survive in these disparate hosts is dependent on the mechanisms to rapidly adapt by sensing the surrounding environment and altering gene expression accordingly (Samuels, 2011; Radolf *et al.*, 2012). While *Escherichia coli* has between 30 to 60 two-component regulatory systems involved in

*Corresponding author: BSE.3.230; Department of Biology, The University of Texas at San Antonio, One UTSA Circle, San Antonio TX-78249. Phone: (210)-458-6679; Fax: (210)-458-5658. j.seshu@utsa.edu.

sensing the environment and regulating genes accordingly, *B. burgdorferi's* genome encodes for only two (Fraser *et al.*, 1997). These systems include the Hpk2-Rrp2 system that regulates RpoS, which in turn regulates many factors required for transmission and vertebrate infection; and Hpk1-Rrp1, which operates through the signaling molecule cyclic di-GMP and regulates metabolic and virulence genes (Hubner *et al.*, 2001; Rogers *et al.*, 2009; Yang *et al.*, 2003; Sultan *et al.*, 2010; Caimano *et al.*, 2011; Samuels, 2011; Radolf et al., 2012).

B. burgdorferi relies intimately on its host for nutrients and metabolites because many biosynthetic genes are absent (Fraser *et al.*, 1997). Many bacteria use nutrients as cues to sense the environment and evidence suggests *B. burgdorferi* uses different carbon sources from each host (Pappas *et al.*, 2011). In other organisms, nutrients stimulate adaptive responses such as proliferation, motility, and virulence factor production (Poncet *et al.*, 2009). Carbohydrate responsive regulators are crucial for relaying these nutrient signals for subsequent modulation of virulence mechanisms (Postma *et al.*, 1993).

Only two carbohydrate responsive regulators are apparent in *B. burgdorferi's* genome, genes *bb0693* and *bb0831*, annotated as xylose operon regulatory proteins (XylR1, XylR2) respectively. XylRs are part of the ROK (repressor, ORF, kinase) family of proteins (Titgemeyer *et al.*, 1994). In addition to XylRs, ROK repressors also include Mlc and NagC in other bacterial systems. Both Mlc and NagC are involved in regulating utilization of phosphotransferase system (PTS) sugars (Plumbridge, 2001). NagC is a dual regulator that represses *nagE-nagBACD* and *chb* operons for n-acetyl-glucosamine (GlcNAc) and chitin/chitobiose catabolism, respectively. In addition, NagC also activates *glmS* operons involved in the biosynthesis of GlcNAc precursors for cell wall biogenesis (Plumbridge & Pellegrini, 2004). Mlc is a global regulator of glucose metabolism and represses *ptsG* and *ptsHI* operons encoding the transporter and cytoplasmic components of the glucose PTS (PTS^{Glc}), respectively (Hosono *et al.*, 1995; Plumbridge, 2002; Schiefner *et al.*, 2005). Mlc also modulates expression of the *chb* operon (Berg *et al.*, 2007). Both Mlc and NagC regulate genes for bacterial virulence. For example, NagC regulates *fimB* recombinase involved in phase variation in Type I fimbriae in *E. coli*, whereas Mlc regulates *Salmonella enterica hilE*, which represses genes in *Salmonella* pathogenicity island I, important for epithelial cell invasion (Poncet *et al.*, 2009; Sohanpal *et al.*, 2007).

Regulation of ROKs involves interaction with their inducing signals. NagC's operons are induced when NagC binds its inducer, GlcNAc-6-phosphate (GlcNAc-6P)(Plumbridge, 1991). In contrast, Mlc is displaced from its operators by sequestration in the inner membrane by binding to the glucose transporting protein PtsG of the PTS^{Glc} (Tanaka *et al.*, 2000).

Given that ROKS play a role in bacterial virulence in other systems, our study aimed to characterize the ROK regulator, XylR1, in *B. burgdorferi*. Our study is the first to demonstrate *B. burgdorferi's* use of a putative carbohydrate responsive regulator and provides a link coordinating host-specific nutrients to host adaptation and thus virulence potential.

RESULTS

Absence of xylose utilization in *B. burgdorferi*

B. burgdorferi has a gene annotated as a xylulokinase (BB0545), but other genes for xylose utilization are absent (Fig. 1A). Previous studies demonstrated glucose, mannose, glycerol, GlcNAc and GlcNAc oligomers (chitin and chitobiose) could all support growth of *B. burgdorferi in vitro*, but not xylose (von Lackum & Stevenson, 2005). This suggests that XylR1 and XylR2 are misannotated, as there appears to be no functional need for regulating xylose utilization in *B. burgdorferi.*

XylRs are included in a family of proteins known as ROKs (repressor, ORF, kinase). Specifically, ROK regulators contain an N-terminal DNA-binding domain, adaptor domain, and a C-terminal sugar-binding domain (Pennetier *et al.*, 2008). The ROK kinases are shorter than the ROK regulators by about 80 residues due to the absence of the N-terminal DNA-binding domain (Titgemeyer *et al.*, 1994). *In silico* analysis of the borrelial XylRs revealed XylR2 has features of a sugar kinase whereas XylR1 demonstrated properties of a transcriptional regulator. XylR2 is lacking the N-terminal DNA-binding domain, whereas this domain is maintained in XylR1.

XylR1 of *B. burgdorferi* shares homology with two other ROK regulatory proteins, NagC (BLASTp=e^{-16}) and Mlc (BLASTp=e^{-14}), involved in regulating GlcNAc and glucose metabolism, respectively. Comparative sequence analysis of the helix-turn-helix motif of the DNA-binding domain demonstrated that XylR1 has many conserved residues found in the other ROKs (e.g. NagC and Mlc of *E. coli* and XylR of *Bacillus subtilis*) (Fig. 1B).

Based on these *in silico* findings, the inability of *B. burgdorferi* to utilize xylose sugars, and several discoveries reported below, we renamed XylR1 as Borrelia host adaptation Regulator (BadR) and will refer to it as such throughout this study.

BadR is elevated in cultures grown under conditions mimicking tick hosts

We hypothesized BadR was a ROK regulator of glucose and/or GlcNAc utilization (e.g. Mlc and/or NagC homolog), as these are sugars utilized by *B. burgdorferi.* We further hypothesized that BadR expression would change in *B. burgdorferi* grown under inducing conditions. In previous studies using qRT-PCR, we found that *badR* transcript levels were negligibly changed in *B. burgdorferi* grown in BSK–Lite media (medium free of supplemental sugars (von Lackum & Stevenson, 2005)) supplemented with various sugars (2X glucose (0.8% w v^{-1}), 2X GlcNAc (0.08% w v^{-1}), 0.4% v v^{-1} glycerol, or 75uM chitobiose) (data not shown). In *E. coli*, NagC is induced only 2-fold by growth under inducing conditions, whereas NagA and NagB expression is induced 20-fold (Plumbridge, 1996). Likewise in *E. coli*, Mlc transcript levels changed less than 2-fold by glucose (Shin *et al.*, 2001). Taken together, these aforementioned studies and the fact that many components in BSK-Lite media are undefined, help explain the negligible changes seen in BadR transcript levels in our sugar-supplemented growth studies.

To assess regulatory targets of BadR, BadR and putative BadR regulated proteins were over-expressed, purified, and used to generate mono-specific anti-sera. Using the antisera

generated, levels of these determinants were observed by immunoblot analysis from borrelial cultures grown under *in vitro* conditions mimicking fed-tick (pH6.8, 37°C) and unfed-tick (pH7.6, 23°C) hosts (Fig. 2A, B). BadR levels were elevated during growth under conditions mimicking the unfed-tick host and displayed opposing trends to the levels of NagC-regulated, GlcNAc catabolic enzymes, NagA (BB0151) and NagB (BB0152), which showed elevated levels under fed-tick growth conditions. Chitobiose transporter subunit, ChbA (BBB05), regulated by both NagC and Mlc in other bacteria, was not preferentially expressed in either host condition. Levels of Mlc-regulated glucose transporter, PtsG (BB0645), were highest in cultures grown under unfed-tick conditions. As a control, we assessed the levels of outer surface protein C, OspC. OspC is a vertebrate-specific determinant, highly up-regulated in spirochetes when the ticks are acquiring a blood meal, and is a critical element for the spirochetes to transmit from the tick to the vertebrate host (Grimm *et al.*, 2004; Pal *et al.*, 2004). OspC levels were highest under conditions mimicking vertebrate hosts indicating proper cell signaling (Fikrig & Narasimhan, 2006). As an additional control, no variations in P66 levels were detected demonstrating equal protein loading.

Taken together, BadR is synthesized at higher levels in the conditions mimicking unfed-ticks. Ticks can persist months between blood meals, so we hypothesize a repressor of sugar utilization genes would be up-regulated because the tick environment is a nutrient limiting state for *B. burgdorferi*. High PtsG levels under unfed-tick growth conditions may illustrate the importance for spirochetes to utilize glucose first, the primary sugar for most microbes, for growth in the tick midgut, which is normally a co-inhabited and thus competitive niche (Benson *et al.*, 2004). Studies have shown that expression of the chitobiose transporter, *chbC* (*bbb04*), is up-regulated under GlcNAc starved *in vitro* growth conditions (Rhodes *et al.*, 2009; Tilly *et al.*, 2001). Other studies found *chbC* transcripts were higher in borrelial cultures grown at 23°C compared to cultures shifted to 34°C. This study also demonstrated that the *chbA* (*bbb05*) and *chbB* (*bbb06*) transcripts were unaffected by this temperature shift (Tilly *et al.*, 2001). The aforementioned studies support our findings regarding ChbA levels (Fig. 2).

Generation and growth phenotype of badR-deficient *B. burgdorferi* B31-A3 strains

To characterize gene regulation attributed to BadR, a *badR*-deficient strain, *badR*$^-$ (Strp^R), was generated in the infectious B31-A3 strain by allelic exchange and confirmed by Southern blot analysis (Fig. 3A, B, and C). In addition, PCR was performed to confirm all essential plasmids were maintained for *B. burgdorferi* to complete the infectious enzootic cycle (Fig. 3D). After numerous attempts to generate a *badR cis*-complemented strain, we decided to generate a second *badR*-deficient strain, *badR2*$^-$ (Gent^R), by allelic exchange using a different antibiotic cassette from *badR*$^-$. The *badR2*$^-$ strain displayed an identical phenotype as *badR*$^-$ (Fig. 4). The *badR*-deficient strains displayed a growth defect under *in vitro* conditions mimicking unfed-tick hosts (Fig. 4B), which suggests a role for BadR in modulating growth kinetics of *B. burgdorferi* during its residence in ticks.

RpoS and vertebrate host-induced factors are up-regulated in badR-deficient strains

To delineate the regulatory role of BadR, the protein profile of the *badR*-deficient strains grown under laboratory conditions (pH7.6, 32°C) was assessed. The *badR*-deficient strains showed negligible changes in NagA, NagB, and PtsG but displayed increases in the levels of chitobiose transporter protein, ChbA, (Fig. 4C, D) suggesting BadR's role in regulating chitobiose metabolism. Intriguingly, *badR*-deficient strains revealed increases in levels of vertebrate-specific factors (e.g. RpoS, BosR, OspC, DbpA) implying BadR's ability to modulate gene expression required for the spirochetes' adaptation to the mammalian host. In addition, our immunoblot analyses demonstrated significant down-regulation of BBI41 levels, an ORF located on linear plasmid 28-4 (lp-28-4), in the *badR*-deficient strains and supported our microarray findings discussed below.

BadR binds to the upstream region of rpoS and binding is alleviated by phosphorylated sugars

To define whether the up-regulation of *rpoS* in the *badR*-deficient strains was a result of indirect mechanisms or by direct regulation of *rpoS* by BadR, DNA-binding assays were performed using recombinant BadR and two *rpoS* promoters. One *rpoS* promoter (P*rpoS*1) included the RpoS start codon and BosR binding site 3 (BS3) (Ouyang *et al.*, 2011). The second *rpoS* promoter (P*rpoS*2) included the RpoN binding site, *rpoS* transcriptional start site, and BosR binding sites 2 and 3 (BS2, BS3) (Fig. 5A). Both promoters, when incubated with BadR, caused a mobility shift and this interaction was outcompeted when 200-fold molar excess of unlabeled promoter was added. A BadR protein lacking the N-terminal helix-turn-helix (HTH) domain (BadRΔHTH) was unable to bind these promoters (Fig. 5B).

We hypothesized BadR may be analogous to NagC which is unable to bind DNA in the presence of the inducer GlcNAc-6P. DNA-binding assays were performed with increasing concentrations of GlcNAc-6P (10-200nmols). Increasing amounts of GlcNAc-6P relieved binding of BadR from P*rpoS*1 and P*rpoS*2 (Fig. 5).

To assess if other sugars were able to inhibit BadR binding, gel mobility shift reactions were performed in the presence of other sugars including: glucose-6P (Glc-6P), xylulose-5P, ribose-5P, xylose, or chitobiose (Fig. 6). Densitometry using ImageJ software assessed inhibition of binding by each sugar (Table S1) (Schneider *et al.*, 2012). The shifted band corresponding to BadR bound to the *rpoS* promoters in the absence of sugars was designated as 100% bound. These studies demonstrated that all phosphorylated sugars inhibited BadR binding to the *rpoS* promoters in a concentration dependent manner, whereas unphosphorylated sugars, such as chitobiose, xylose, and acetate (data not shown), did not disrupt DNA binding (Fig. 6).

Site-directed mutations in BadR affect its binding to rpoS

To further characterize the ROK regulator, site-directed mutants of BadR were generated for use in mobility shift assays using the *rpoS* promoters. *E. coli* Mlc and NagC ROK regulators share residues thought to be important for binding their inducer, which include: H194, D195, E244, H247, and E266 (Mlc numbering; Fig. 7A, B) (Pennetier *et al.*, 2008). Of these residues, BadR maintains only H247, which corresponds to H243 in Figure 7B. Consistent

with the phenotype observed with *E. coli* NagC and Mlc H247 mutants, BadR with a H243A substitution was unable to bind to the *rpoS* promoter, which suggests H243 may also be critical for DNA binding of BadR (Fig. 7C, lane 5). Mutations in H194, E244, E266, and G246 in the *E. coli* NagC resulted in proteins insensitive to their inducer, GlcNAc-6P (Pennetier *et al.*, 2008). Since BadR does not maintain any of these conserved residues, we focused on BadR-unique residues. *In silico* analyses utilizing the UniProtKB/Swiss-Prot database, suggested acetate could serve as a putative ligand of BadR. Acetate's conversion to acetyl-P plays a crucial role in triggering vertebrate specific adaptation (Fig. 8C) (Raju *et al.*, 2011; Van Laar *et al.*, 2012; Sze & Li, 2011). Therefore, we decided to mutate N253 and P256 residues in BadR's inducer binding domain (IBD) because previous studies identified N91 and P232 as crucial residues in mediating acetate kinase's ability to bind acetate in *Methanosarcina thermophila* (Ingram-Smith *et al.*, 2005). N253A/P256A BadR mutant bound to the *rpoS* promoter (Fig. 7C, lane 7) and responded to various sugars similarly as the WT (Fig. S1 and Table S2). The last 18 amino acids of *E. coli* Mlc are critical in orienting the HTH domain to facilitate DNA binding (Schiefner *et al.*, 2005). Removal of the entire IBD C-terminal domain yielded a mutant BadR unable to bind the *rpoS* promoter (Fig. 7C, lane 4). Mutations in the putative dimerization/metal binding residues (C254, C257) also prevented BadR from binding to the *rpoS* promoter (Fig. 7C, lane 6) and parallels results seen in equivalent Mlc mutants in *E. coli.* Ultimately, this demonstrated that C254 and C257 may also play a structural role and contribute to orientation of the HTH domain in BadR (Schiefner *et al.*, 2005). Taken together, BadR has several residues important for function that are shared with both Mlc and NagC.

Up-regulation of vertebrate-specific determinants and down-regulation of tick-specific determinants in badR-deficient strains

To identify, further, BadR's regulatory network, *badR*$^{-}$ and parental WT were compared using microarray analyses of these cultures grown under laboratory growth conditions (pH7.6, 32°C). Two independent but identically designed microarrays were performed and results were consistent with our immunoblot findings (e.g. up-regulation of chitobiose utilization genes in *badR*$^{-}$) (Table 1, and accession GSE38827). To validate our microarray, quantitative RT-PCR was performed on a handful of transcripts (Table 2 and Fig. 8). Table 1 demonstrates data derived from both microarrays and specifically displays genes with at least a 2-fold difference in gene expression when comparing *badR*$^{-}$ to WT strains. Approximately one-third (39%) of the genes displayed in Table 1 were down-regulated in *badR*$^{-}$ compared to WT. Among those down-regulated genes, a large proportion (43% and 29%) was present on the chromosome and lp28-4, respectively. The majority of these down-regulated genes (63%) are annotated as hypothetical proteins. Approximately two-thirds (62%) of the genes displayed in Table 1 were up-regulated in *badR*$^{-}$ compared to WT. Among those up-regulated genes, most (38% and 17%) were present on circular plasmids 32 (cp32 1-4) and the chromosome, respectively. The majority (65%) of these up-regulated genes are annotated as hypothetical proteins. Intriguingly, *badR*$^{-}$ displayed up-regulation of *rpoS*, as well as genes regulated by the Rrp^{2}-RpoN-RpoS pathway, such as *ospC, dbpA, dbpB*, *bba07*, *bba64*, and *bb844*. Other factors important for virulence in vertebrate hosts including antigens recognized by Lyme disease patient sera (e.g. BBP28 (*mlp*), BBI42,

BBQ47 (*erpX*), BBS41 (*erpG*), BBO39 (*erpL*), BBG23, and BBQ03) were also up-regulated in *badR*¯ (Xu *et al.*, 2008) (Fig. 8, Table 1, and Table 2).

BadR binds to the same promoter as BosR in our DNA-binding assays. Ouyang *et al.* predicted additional putative BosR-regulated promoters (Ouyang *et al.*, 2011). Interestingly, 25% of the putative BosR-regulated genes displayed significant expression changes in *badR*¯ including: *bb0020* (*pfpB*), *bb0055* (*tpi*), and *bbb29 (malX*), a PtsG homolog (Table 1, and accession GSE38827).

Collectively, these results suggest BadR functions as a versatile ROK regulator, regulating both chitobiose utilization and genes required for host adaptation (e.g. *rpoS*). BadR may also interplay with BosR at various gene targets. Our results demonstrate a regulatory network unique to *B. burgdorferi* pathogenesis, because a significant proportion of differentially expressed genes in *badR*¯ encode hypothetical proteins of unknown function and located on replicon, lp28-4; a plasmid shown to be important for the spirochete's survival in ticks (Strother *et al.*, 2005; Elias *et al.*, 2002).

BadR is required for mammalian infectivity

To determine if BadR is critical for *B. burgdorferi* to infect the mammalian host, C3H/HeN mice were infected with 10^5 *B. burgdorferi* strains by needle inoculation. Fourteen days post infection the *badR*-deficient strains were not isolated from any of the infected tissues, while the wild-type parental strain, B31-A3, could be isolated from all the tissues tested (Table 4). Since *badR*-deficient strains display increased expression of outer surface antigens (e.g. OspC and DbpA) which might enhance bacterial clearance, immunodeficient SCID mice were also infected with 10^5 spirochetes. Similarly, *badR*-deficient *B. burgdorferi* could not be propagated from the infected tissues of SCID mice 14 days post infection. Since the innate immune system of SCID mice is still intact, it is possible that key components of innate immunity (e.g. complement) play a role in the clearance of the *badR*-deficient strains. Moreover, other mechanisms responsible for the unsuccessful colonization, dissemination, and survival of these mutant strains in mammalian hosts cannot be ruled out. Taken together, BadR is critical for *B. burgdorferi* to colonize mammalian hosts.

DISCUSSION

BadR repression of RpoS

For the host-propagated pathogen *B. burgdorferi*, adaptive phenotypic changes required to switch between its two hosts is energetically expensive and resembles an all-or-none response. At some point, there is a crucial signal that triggers the spirochetes to commit, spend energy, and undergo these adaptive changes. The transcription factor RpoS has been termed the "gatekeeper" because it promotes rapid adaptation as it expresses the genes required for *B. burgdorferi* to transmit to and infect vertebrate hosts (Caimano *et al.*, 2007; Dunham-Ems *et al.*, 2012; Ouyang *et al.*, 2012). Understandably, expression of *rpoS* is a committed step that must be appropriately regulated. A slew of studies have identified factors that activate *rpoS*, but there is a dearth of information on how *rpoS* is repressed to down-regulate vertebrate-specific adaptations, to allow *B. burgdorferi's* transition back into

ticks. While a reduction in intensity of external signals that lead to *rpoS* activation is one possibility, our study found that the transcriptional regulator BadR mediates *rpoS* repression by binding upstream regions of *rpoS* directly (Fig. 8C).

Intriguingly, the phenotype of *badR*-deficient strains is an increase in expression and level of *rpoS* and RpoS-regulated genes. Generally, expression of *rpoS* is mediated by the alternative σ factor RpoN. However RpoN-independent *rpoS* activation has also been suggested to occur through σ^{70} factor, RpoD (Samuels, 2011). Increased temperatures from blood meals promotes a small RNA, $DsrA_{Bb}$, to unfold and promote RpoS translation from a longer *rpoS* mRNA, transcribed with the aid of RpoD (Lybecker & Samuels, 2007). Previous studies have shown acetyl phosphate (elevated due to inhibitory effects of Carbon Storage Regulator A ($CsrA_{Bb}$) on phosphate acetyl-transferase (Pta)), phosphorylates and activates Rrp2, an enhancer binding protein which activates RpoN dependent transcription of *rpoS* (Karna *et al.*, 2011; Sze *et al.*, 2011). Borrelia oxidative stress regulator, BosR, also binds to upstream regions of *rpoS* and enhances *rpoS* expression (Ouyang *et al.*, 2011; Hyde *et al.*, 2006). It is plausible that the high RpoS levels and transcripts in a *badR*-deficient strain could be a consequence of modulating any one of these processes; however, our findings support the hypothesis that BadR is a direct transcriptional repressor of *rpoS*.

First, our microarray analyses did not reflect significant increases in expression of *rrp2, rpoN, rpoD,* $dsrA_{Bb}$, $csrA_{Bb}$, *bosR*, or acetate metabolic enzymes, *pta* and *ackA*, in $badR^{-}$, suggesting increases in *rpoS* could not be attributed to BadR's transcriptional regulation of these factors. To further support that BadR is a direct transcriptional repressor of *rpoS*, we found elevated levels of BadR in A3 WT grown under unfed-tick conditions where there is little or no RpoS levels. Furthermore, we found increases in both *rpoS* transcripts and RpoS levels in the *badR*-deficient strains compared to WT. We do understand, however, that these are *in vitro* conditions and the repression of *rpoS* by BadR needs to be addressed in future *in vivo* studies. Finally, to further support that BadR is a direct transcriptional repressor of *rpoS*, BadR bound to two regions upstream of *rpoS in vitro.*

Taken together, BadR appears to repress *rpoS* expression presumably by means of excluding the binding of *rpoS* activators, e.g. BosR, RpoN, and/or RpoD. Additionally, since BadR is a ROK family member comprised of regulators that are responsive to carbohydrates and typically bind sugars to modulate their regulatory function, we predict that BadR's repression of *rpoS* is alleviated through its direct or indirect interaction with an inducing signal, probably a sugar or byproduct linked to nutrient metabolism (Fig. 8C).

ROK Regulators: Modulators of Virulence Potential

badR-deficient *B. burgdorferi* strains were completely unable to establish infection in both immunocompetent (C3H/HeN, BALB/c) and immunodeficient mice (SCID), indicating BadR is an important regulator of *B. burgdorferi* virulence. Microarray analyses revealed that BadR regulates the transcription of virulence genes. In the *badR*-deficient strains, there was an up-regulation of *rpoS*, the genes regulated by the Rrp2-RpoN-RpoS pathway, as well as other vertebrate specific factors important for virulence (e.g. antigens recognized by the sera of Lyme disease patients).

B. burgdorferi strains carry up to ten cp32 plasmids and numerous questions remain unanswered regarding cp32 genes and the role of their encoded proteins in pathogenesis (Stevenson *et al.*, 2000; Kenedy *et al.*, 2012). Because approximately one-third of genes up-regulated were from cp32 plasmids and approximately two-thirds of differentially expressed genes, both up- and down-regulated, were annotated as hypothetical proteins of unknown function in *badR*$^{-}$, we suggest a number of these genes are likely critical for *B. burgdorferi* pathogenesis and virulence.

ROKs can function as both repressors and activators (Plumbridge, 1995). Our results imply BadR is an activator of tick-specific factors because *badR*$^{-}$ had significant decreases in expression of genes encoded on lp28-4. Previous studies found that *B. burgdorferi* strains absent of lp28-4 were unable to be transmitted from ticks to naïve mice and overall had reduced infectivity of tick midguts (Strother *et al.*, 2005; Elias *et al.*, 2002). Therefore, it has been hypothesized that lp28-4 is important for *B. burgdorferi's* residence in the tick, specifically flat ticks and hence nutrient depleted environments (Tokarz *et al.*, 2004). Consistent with this observation, our microarray showed down-regulation of guanosine-3′, 5′-bis (diphosphate) 3′-pyrophosphohydrolase (Rel_{Bbu}) in the *badR*$^{-}$ strain. Rel_{Bbu} is up-regulated during starvation and important for *B. burgdorferi* to adapt to stationary phase (Bugrysheva *et al.*, 2005). Collectively, BadR positively regulates genes most likely important for the survival of spirochetes in the nutrient-limiting environments within the tick (Fig. 8C). Therefore, we hypothesize that *badR*-deficient strains will also have reduced infectivity in ticks and we will assess this in future *in vivo* studies.

The ability of BadR to repress vertebrate-specific virulence factors while simultaneously activating the expression of tick-specific factors demonstrates a central role of this regulator in the lifecycle of *B. burgdorferi*. We suggest that the dysregulation of these host-specific factors within the *badR*$^{-}$ mutant is the cause of the high level of attenuation seen in this strain in mice.

ROK Regulators: Modulated by Nutrients

Many studies highlight food availability as the principle factor for microbes to adapt and survive, as well as provide the evolutionary push for the development of pathogenic characteristics (Poncet *et al.*, 2009). We investigated whether host-specific nutrients contribute to *B. burgdorferi's* pathogenesis. Our study aimed to characterize the only apparent carbohydrate responsive regulatory protein, a gene we have renamed BadR. BadR is a ROK family member, which includes repressors such as NagC, Mlc, and XylR involved in regulating GlcNAc, glucose, and xylose metabolism, respectively. *B. burgdorferi* does not utilize xylose but does utilize GlcNAc and glucose sugars. Many bacteria have multiple ROK regulators, specific for each sugar utilized (Titgemeyer *et al.*, 1994). Interestingly, this is not the case with *B. burgdorferi* as BadR is the only ROK regulator identified in the genome. Since the *B. burgdorferi* genome has few transcriptional regulators, this suggests that these regulators are versatile and lead us to hypothesize BadR is a unique ROK regulator, unlike NagCs and Mlcs in other systems, and to which our findings support.

First, BadR's original annotation as a XylR1 would imply its regulation is through the binding of xylose, but xylose had no effect on the binding of BadR to the *rpoS* promoters.

Secondly, the *badR*-deficient strains displayed a significant up-regulation of chitobiose utilization genes, suggesting BadR functions similar to NagC and Mlc, because both modulate expression of these genes in other bacteria (Berg *et al.*, 2007; Plumbridge & Pellegrini, 2004). BadR is unlike a NagC, however, because levels of catabolic enzymes, NagA and NagB, were not affected in *badR*-deficient strains; whereas a *nagC*-deficient *E. coli* demonstrates a 20-fold induction of *nagB* (Plumbridge, 1991). On the other hand, BadR is like a NagC in that GlcNAc-6P disrupted BadR's binding to the *rpoS* promoters. However, our studies demonstrated that several phosphorylated sugars (e.g. GlcNAc-6P, Glc-6P, ribose-5P) disrupted the binding of BadR to the *rpoS* promoter.

Site-directed mutants of BadR were generated in the putative inducer/sugar binding domain (IBD) to generate a mutant BadR unresponsive to its inducer, which would aid in identifying any specific interactions with the sugars and BadR. Previous studies identified residues in both NagC and Mlc proteins in *E. coli* that when mutated result in regulators insensitive to their inducer (Pennetier *et al.*, 2008). However, BadR does not maintain any of these conserved residues, further illustrating its unique qualities. A couple of residues that were mutated in the IBD domain of BadR had no effect on BadR binding to the *rpoS* promoter in the presence of various sugars. Removal of the entire IBD domain yielded a BadR protein unable to bind to the *rpoS* promoters and is consistent with *E. coli* Mlc mutants lacking the last 18 amino acids (Schiefner *et al.*, 2005).

BadR's regulatory function may not be modulated like NagCs and XylRs, which are directly bound by their specific sugar/inducer. It is feasible that BadR is similarly regulated as an Mlc, specifically being sequestered in the inner membrane through its binding of the PTS transporter protein, PtsG. Mlc-deficient strains of *E. coli* display a modest 2-fold induction of *ptsG* (Plumbridge, 2001; Kimata *et al.*, 1998). Even though our study did not address spatial location of BadR in the presence or absence of these sugars, *badR*$^{-}$ did not show a significant induction of *ptsG* transcript, suggesting that BadR is unlike an Mlc.

Further structure/function studies of mutant BadR proteins gave more insight into the characteristics of BadR. We analyzed the effects of site-specific changes in residues conserved in BadR that have been shown to be important for the function of both Mlc and NagC in *E. coli*. First, C254A/C257A (putative metal binding residues) and H243A BadR mutants were unable to bind the *rpoS* promoter and parallels results seen in equivalent Mlc and NagC mutants in *E. coli* (Pennetier *et al.*, 2008).

Taken together, BadR has many characteristics similar to Mlc and NagC but our results suggest BadR is a unique ROK regulator. Our study did not identify a specific inducer of BadR, however, it cannot be ruled out that phosphorylated sugars may serve as inducing signals for BadR *in vivo*. In general, *B. burgdorferi* has a limited genome with limited metabolic capabilities, so perhaps BadR has evolved to recognize multiple phospho-sugars because it functions in place of multiple regulators found in other bacteria. Nevertheless, we postulate that under conditions encountered within different host environments, BadR modifies its regulatory function at its various gene targets through its interaction with host-specific nutrients or by collaboration with other proteins or regulatory elements (Jutras *et al.*, 2012).

ROK Regulators: Modulators of Metabolism

BadR negatively regulates chitobiose transporter genes (*chbA, chbB, chbC*) indicated by the up-regulation of these genes in the *badR*-deficient strains. Chitobiose, a GlcNAc dimer, constitutes the subunit of chitin, which is an abundant component found only in ticks and not in mammals. Evidence supports that chitin and chitobiose (GlcNAc dimer) alone can provide the GlcNAc source to support growth of *B. burgdorferi in vitro* (Tilly *et al.*, 2001). Interestingly, a *chbC*-deficient borrelial strain demonstrated ChbC was not essential for any stage of the mouse-tick-mouse infection model (Tilly *et al.*, 2004; Tilly *et al.*, 2001).

Nevertheless, it has been hypothesized that expression of these genes may enhance bacterial survival in nutritionally stressful circumstances (Tilly *et al.*, 2001; Tilly *et al.*, 2004; Rhodes *et al.*, 2010; Rhodes *et al.*, 2009). However, studies suggest that the presence of exogenous chitobiose is not sufficient to induce the expression of the chitobiose transport genes. *chbC* transcripts are not induced from *B. burgdorferi* cultures grown in media supplemented with chitobiose (Tilly *et al.*, 2001), and ChbC levels remain low in the presence of free GlcNAc (Rhodes *et al.*, 2009; Tilly *et al.*, 2001). We postulate that the presence of an inducer molecule for BadR may be only one requirement necessary to facilitate expression of the chitobiose utilization genes, similar to *E. coli*, in which expression of *chbC* is regulated by NagC as well as two additional regulatory proteins, ChbR and CAP (Plumbridge & Pellegrini, 2004).

Conclusion

Our findings suggest that the transcriptional regulator, BadR, is a key component in the lifecycle of *B. burgdorferi* because it simultaneously activates genes important for the tick-specific lifestyle while repressing genes critical for vertebrate-specific infection. Its repressive effects on mammalian-specific virulence factors could be traced to regulation of the "gatekeeper," *rpoS*; BadR binds to the *rpoS* promoter and represses its transcription. Since ROK regulators, including BadR, are typically modulated through their direct interactions with carbohydrates or byproducts of metabolism, influx of vertebrate-specific sugars may be a trigger that induces the RpoS-dependent expression of virulence factors upon entry of *B. burgdorferi* into the mammalian host. Our results also imply that BadR is an activator of tick determinants such as chitobiose utilization genes and genes of lp28-4, which are thought to be involved in *B. burgdorferi's* maintenance in ticks. Thus, BadR is a critical regulator that most likely couples nutrient availability to niche-specific gene expression, allowing appropriate adaptation to both the tick and vertebrate environments. This study is the first to identify and characterize this novel regulator in *B. burgdorferi*, and reveals novel targets to reduce the transmission and incidence of Lyme disease (Fig. 8).

EXPERIMENTAL PROCEDURES

Recombinant proteins and antibody production

Recombinant proteins and monospecific sera were generated as previously described (Karna *et al.*, 2011; Esteve-Gassent *et al.*, 2009; Van Laar *et al.*, 2012). Briefly, total genomic DNA obtained from *B. burgdorferi* clonal isolate MSK5 was used as a template to PCR amplify genes previously discussed and using primers listed in Table S3. Amplified genes were

cloned into the inducible protein expression vector pET23a (Novagen). *E. coli* expression host Rosetta™ (Novagen) were transformed with the expression vector and induced with 1mM IPTG. Recombinant proteins were gel purified using the ELUTRAP System (Whatman). Six to eight weeks-old female BALB/c mice (n=5) were immunized subcutaneously with 50–100 μg of protein with equal proportion of adjuvant, TiterMax™ (Sigma) in phosphate saline buffer. Boosters were given at day 14 and 21 and immune serum from blood was collected on day 28.

For recombinant proteins used in the EMSAs, amplified products of full-length *badR* and a *badR* amplicon lacking the N-terminal helix-turn-helix domain or the C-terminal putative sugar/inducer binding domain were subsequently cloned into the pMAL-c2X expression vector (New England Biolabs). This vector facilitates the generation of recombinant proteins fused to an N-terminal maltose binding protein. Site directed mutagenesis of the BadR protein was performed to replace conserved (H243, and C254/C257 simultaneously-putative dimerization domain) and unique residues of BadR (N253/P256 simultaneously) to alanines. The pMAL-c2X expression vector containing the WT *badR* gene was used as the template using Quick Change Site-Directed Mutagenesis Kit (Stratagene) and the designated primers (Table S3). Plasmids were screened by restriction enzymes and sequenced. Rosetta™ (Novagen) cells were transformed and allowed to reach logarithmic phase at 37°C. Cells were allowed to induce overnight at 16°C (1mM IPTG), collected by centrifugation, and resuspended in 30ml of low salt buffer (LSB; 10mM phosphate, 30mM NaCl, 10mM β-ME, 1mM EGTA, pH 7.0). The cells were lysed by French press (1000 psi), centrifuged, and supernatants were loaded onto an amylose column for purification using the Biologic Duo-Flow FPLC (Bio-Rad) as per manufactures instructions. Proteins were stored at −80°C and concentrations were determined using Bio-Rad protein assay with BSA as a standard (Bio-Rad).

Bacterial strains and growth conditions

Strains utilized in this study are listed in Table 3. Briefly, infectious *B. burgdorferi* strain, B31-A3, was cultured in Barbour-Stoenner-Kelly (BSK)-II medium with 6% rabbit serum (Pel-Freez) at 32°C or 37°C in a CO_2 (1%) incubator or at 23°C and grown to 5×10^7 bacteria ml^{-1} as previously described (Van Laar *et al.*, 2012; Karna *et al.*, 2011; Esteve-Gassent *et al.*, 2009). For growth curves, spirochetes were diluted from stationary phase (1×10^8 bacteria ml^{-1}) and seeded at 5×10^5 bacteria ml^{-1} into 10 ml cultures in BSK-II medium supplemented with 6% NRS (for all strains), 100μg ml^{-1} of streptomycin (for *badR*$^-$) and 40μg ml^{-1} of gentamycin (*badR2*$^-$). Cells were enumerated every 24 hours for cultures grown at 32°C and 23°C using dark field microscopy. The cultures were grown in triplicate, with three independent trials. Levels of significance were determined using GRAPHPAD PRISM v.4.0 (Graph Pad Software) and two-way ANOVA with α=95%.

Generation of badR-deficient B31-A3 strain

A suicide vector was generated, as previously described (Karna *et al.*, 2011), which allowed for deletion of the *badR* gene through allelic exchange with an antibiotic cassette, $P_{flgB}Str^R$ or $P_{flgB}Gent^R$, for the first and second *badR*-deficient strain, respectively. Primers used are listed in Table S3. The antibiotic cassettes were driven by a constituently expressed borrelial

promoter, P_{flgB}. Briefly, ~1-kb regions of the borrelial chromosome flanking the badR gene were PCR amplified from total genomic DNA from infectious, clonal isolate of *B. burgdorferi* B31-A3. In the second step, a ~2-kb amplicon was PCR amplified by LATaq polymerase (Takara) using the PCR products from the first step as DNA templates. The amplicon was cloned into pCR2.1 cloning vector (Invitrogen) and transformed into TOP 10 *E. coli*. A plasmid with an appropriate insert was identified following blue/white screening, and the antibiotic cassette was cloned into this plasmid using the SalI sites present on the primers used. The final plasmid used for the generation of the mutant in the infectious strain of *B. burgdorferi* B31-A3 is illustrated in Fig. 3 (Samuels, 1995).

The transformants were plated on BSK-II agarose overlays and counter selected in the presence of streptomycin or gentamycin (100μg ml^{-1} or 40μg ml^{-1}, respectively). Plates were incubated at 32°C in 1% CO_2 until individual colonies were visible, at which then they were isolated aseptically into BSK-II liquid medium and incubated at 32°C until the spirochetes reached a density of 5×10^7 ml^{-1}. Total genomic DNA was extracted from this culture and the presence of the antibiotic cassettes was determined by PCR. A positive clone was further confirmed for the loss of *badR* by Southern blot and immunoblot analysis.

Southern blot analysis

As described previously (Raju *et al.*, 2011), total genomic DNA was extracted from WT and *badR*$^-$ strains, digested with various restricted enzymes, separated on a 1% agarose gel, and transferred onto a Nylon membrane (Amersham Hybond-N+;GE Healthcare). PCR amplified probes corresponding to the *aadA* gene (Str^R maker) or to a region upstream of the *badR* gene were labeled using the Enhanced Chemiluminescence Labeling and Detection System (GE Healthcare). Membranes were hybridized with the probes overnight at 42°C, washed, and developed according the manufacturer's protocol.

SDS-PAGE and immunoblot analyses

Whole-cell *B. burgdorferi* lysates were prepared, separated on SDS-PAGE, and visualized either by Coomassie brilliant blue staining or transferred onto PVDF membranes for immunoblot analysis, as previously described (Van Laar *et al.*, 2012; Sanjuan *et al.*, 2009). Equivalent loading of protein was estimated with Coomassie blue staining and immunoblot analysis with mouse anti-P66 serum. The PVDF membranes were blocked with 1% non-fat milk, and probed with mouse, rat, or rabbit antibodies against aforementioned antigens. Subsequent probing with appropriate dilutions of horse radish peroxidase-conjugated anti-mouse, anti-rat, or anti-rabbit serum allowed for visualization using ECL Western blotting reagents (GE Healthcare).

RNA extraction and quantitative RT-PCR

Procedures were as previously described (Karna *et al.*, 2011). WT parental A3 strain and the *badR* deficient mutant were grown in BSK-II at 32°C until cultures reached mid-logarithmic phase corresponding to $5{\times}10^7$ cells ml^{-1}. RNA was harvested using RNA-Bee (Tel-Test, Inc.) and phenol/chloroform followed by isopropanol precipitation and washes with 75%ethanol. Genomic DNA was removed by treatment with DNAse I. RNA was quantified using the Nanodrop spectrophotometer (Invitrogen) and absence of DNA contamination was

confirmed using PCR primers specific for the *recA* gene in *B. burgdorferi.* The RNA was reverse transcribed to cDNA using TaqMan reverse transcription reagents (Applied Biosystems). Quantitative real-time PCRs was performed using SYBR green master mix (Ambion) with specified primers (Table S3) and analysis by ABI Prism 7300 system (Applied Biosystems) with relative changes using *recA* for normalization and fold difference with $2^{-\Delta\Delta Ct}$ method. Unpaired student's t-test and $P<0.05$ (Prism) were implemented.

Microarray analyses

RNA from cultures grown under pH7.6/32°C was harvested as previously described, (Karna *et al.*, 2011), and sent to Roche Nimblegen for cDNA synthesis and microarray hybridization. Two separate but identically designed microarrays were performed. Microarray data deposited in NCBI's Gene Expression Omnibus (Edgar *et al.*, 2002) and are accessible through GEO Series accession number GSE38827 (http://www.ncbi.nlm.nih.gov/geo/query/acc.cgi?acc=GSE38827). Hierarchical clustering and correlation analysis was used to verify quality of the normalized array data. The expression data from biological replicates 1 and 2 were both pooled and analyzed individually. We used LIMMA R package to test contrasts between WT and *badR*-deficient strains (Smyth, 2004). We reported raw and log2 fold change (*rpoS*; Fig. 8), and computed 95% confidence intervals, p-value, and adjusted Benjamini-Hochberg False Discovery Rates (FDR). Genes ≥2 fold differences in expression and overall $P\leq0.05$ were reported (Table 1).

EMSAs

Primers used are listed (Table S3). 5′ biotinylated promoters were produced by Nucleic Acids Core Facility (University of Texas Health Science Center, SA, TX) and purified (SV gel-PCR cleanup-Promega). LightShift Chemiluminescent EMSA kit was utilized according to manufacturer's recommendations (Pierce Biotechnology). Briefly, labeled promoters (1.9 nmols) and BadR (135, 205, or 270 pmols) were mixed in 20μl buffer (10mM Tris (pH7.5), 50mM KCl, 1mM DTT, and 2ug poly(dI-dC) for 20 min at 23°C, run on 6% polyacrylamide gel, transferred onto Nylon membranes (GE Healthcare), UV-cross-linked, and visualized with LightShift reagents. Some reactions included GlcNAc-6P, glucose-6P (Glc-6P), xylulose-5P, ribose-5P, xylose, or chitobiose (10, 30, 50, 100, or 200mM; Sigma-Aldrich) and unlabeled promoters (200-fold molar excess), for induction and competition studies, respectively. Densitometry to assess inhibition of binding by sugars was performed using ImageJ software (Table S1 and S2) (Schneider *et al.*, 2012). A representative experiment was shown. The shifted band corresponding to BadR's binding to the *rpoS* promoters in the absence of sugars was designated as a 100% bound.

Infectivity Analysis

Six-week old female C3H/HeN, SCID, or BALB/c mice were inoculated intradermally with 10^5 spirochetes per mouse with the following borrelial strains: wild-type (B31-A3), *badR*-deficient strain 1 (*badR1*$^-$) and *badR*-deficient strain 2 (*badR2*$^-$). Fourteen days after inoculation, the spleen, left-tibiotarsal joint, left inguinal lymph node, heart, bladder and a piece of abdominal skin were collected, and cultured in BSK-II growth medium to facilitate isolation of spirochetes as previously described. The cultures were scored for growth of *B. burgdorferi* after 2 to 3 weeks using dark field microscopy (Table 4). All animal procedures

were performed in accordance with the animal use protocol approved by Institutional Animal Care and Use Committee (IACUC) at the University of Texas at San Antonio.

Supplementary Material

Refer to Web version on PubMed Central for supplementary material.

Acknowledgments

We thank Patti Rosa for *B. burgdorferi* strain B31-A3. The research was partly funded by Public Health Service Grant SC1-AI-078559 from the NIH-NIAID, the Army Research Office of DoD under Contract No: W911NF-11-1-0136, pre-doctoral fellowships from CEIG (CLM) and STCEID (SLRK). We thank Dr. J.A.L. Gelfond, UTHSC, Epidemiology & Biostatistics, San Antonio, TX, for his expertise and statistical analyses of our microarray studies. We thank Karl E. Klose and M. Neal Guentzel for critically reading the manuscript.

References

Barbour AG, Burgdorfer W, Grunwaldt E, Steere AC. Antibodies of patients with Lyme disease to components of the *Ixodes dammini* spirochete. J Clin Invest. 1983; 72:504–515. [PubMed: 6348092]

Benson MJ, Gawronski JD, Eveleigh DE, Benson DR. Intracellular symbionts and other bacteria associated with deer ticks (*Ixodes scapularis*) from Nantucket and Wellfleet, Cape Cod, Massachusetts. Appl Environ Microbiol. 2004; 70:616–620. [PubMed: 14711698]

Berg T, Schild S, Reidl J. Regulation of the chitobiose-phosphotransferase system in *Vibrio cholerae*. Arch Microbiol. 2007; 187:433–439. [PubMed: 17277949]

Bugrysheva JV, Bryksin AV, Godfrey HP, Cabello FC. *Borrelia burgdorferi rel* is responsible for generation of guanosine-3′-diphosphate-5′-triphosphate and growth control. Infect Immun. 2005; 73:4972–4981. [PubMed: 16041012]

Caimano MJ, Iyer R, Eggers CH, Gonzalez C, Morton EA, Gilbert MA, et al. Analysis of the RpoS regulon in *Borrelia burgdorferi* in response to mammalian host signals provides insight into RpoS function during the enzootic cycle. Mol Microbiol. 2007; 65:1193–1217. [PubMed: 17645733]

Caimano MJ, Kenedy MR, Kairu T, Desrosiers DC, Harman M, Dunham-Ems S, et al. The hybrid histidine kinase Hk1 is part of a two-component system that is essential for survival of *Borrelia burgdorferi* in feeding *Ixodes scapularis* ticks. Infect Immun. 2011; 79:3117–3130. [PubMed: 21606185]

CDC. Summary of notifiable diseases–United States,2010. MMWR Morb Mortal Wkly Rep. 2012; 59:1–111. [PubMed: 22647710]

Dunham-Ems SM, Caimano MJ, Eggers CH, Radolf JD. *Borrelia burgdorferi* requires the alternative sigma factor RpoS for dissemination within the vector during tick-to-mammal transmission. PLoS Pathog. 2012; 8:e1002532. [PubMed: 22359504]

Edgar R, Domrachev M, Lash AE. Gene Expression Omnibus: NCBI gene expression and hybridization array data repository. Nucleic Acids Res. 2002; 30:207–210. [PubMed: 11752295]

Elias AF, Schmutzhard J, Stewart PE, Schwan TG, Rosa P. Population dynamics of a heterogeneous *Borrelia burgdorferi* B31 strain in an experimental mouse-tick infectious cycle. Wien Klin Wochenschr. 2002; 114:557–561. [PubMed: 12422601]

Elias AF, Stewart PE, Grimm D, Caimano MJ, Eggers CH, Tilly K, et al. Clonal polymorphism of *Borrelia burgdorferi* strain B31 MI: implications for mutagenesis in an infectious strain background. Infect Immun. 2002; 70:2139–2150. [PubMed: 11895980]

Esteve-Gassent MD, Elliott NL, Seshu J. *sodA* is essential for virulence of *Borrelia burgdorferi* in the murine model of Lyme disease. Mol Microbiol. 2009; 71:594–612. [PubMed: 19040638]

Fikrig E, Narasimhan S. *Borrelia burgdorferi*–traveling incognito? Microbes Infect. 2006; 8:1390–1399. [PubMed: 16698304]

Fraser CM, Casjens S, Huang WM, Sutton GG, Clayton R, Lathigra R, et al. Genomic sequence of a Lyme disease spirochaete, *Borrelia burgdorferi*. Nature. 1997; 390:580–586. [PubMed: 9403685]

Grimm D, Tilly K, Byram R, Stewart PE, Krum JG, Bueschel DM, et al. Outer-surface protein C of the Lyme disease spirochete: a protein induced in ticks for infection of mammals. Proc Natl Acad Sci U S A. 2004; 101:3142–3147. [PubMed: 14970347]

Hosono K, Kakuda H, Ichihara S. Decreasing accumulation of acetate in a rich medium by *Escherichia coli* on introduction of genes on a multicopy plasmid. Biosci Biotechnol Biochem. 1995; 59:256–261. [PubMed: 7766024]

Hubner A, Yang X, Nolen DM, Popova TG, Cabello FC, Norgard MV. Expression of *Borrelia burgdorferi* OspC and DbpA is controlled by a RpoN-RpoS regulatory pathway. Proc Natl Acad Sci U S A. 2001; 98:12724–12729. [PubMed: 11675503]

Hyde JA, Seshu J, Skare JT. Transcriptional profiling of *Borrelia burgdorferi* containing a unique *bosR* allele identifies a putative oxidative stress regulon. Microbiology. 2006; 152:2599–2609. [PubMed: 16946255]

Ingram-Smith C, Gorrell A, Lawrence SH, Iyer P, Smith K, Ferry JG. Characterization of the acetate binding pocket in the *Methanosarcina thermophila* acetate kinase. J Bacteriol. 2005; 187:2386–2394. [PubMed: 15774882]

Jutras BL, Bowman A, Brissette CA, Adams CA, Verma A, Chenail AM, et al. EbfC (YbaB) is a new type of bacterial nucleoid-associated protein, and a global regulator of gene expression in the Lyme disease spirochete. J Bacteriol. 2012

Karna SL, Sanjuan E, Esteve-Gassent MD, Miller CL, Maruskova M, Seshu J. CsrA modulates levels of lipoproteins and key regulators of gene expression critical for pathogenic mechanisms of *Borrelia burgdorferi*. Infect Immun. 2011; 79:732–744. [PubMed: 21078860]

Kenedy MR, Lenhart TR, Akins DR. The role of *Borrelia burgdorferi* outer surface proteins. FEMS Immunol Med Microbiol. 2012; 66:1–19. [PubMed: 22540535]

Kimata K, Inada T, Tagami H, Aiba H. A global repressor (Mlc) is involved in glucose induction of the *ptsG* gene encoding major glucose transporter in *Escherichia coli*. Mol Microbiol. 1998; 29:1509–1519. [PubMed: 9781886]

Lybecker MC, Samuels DS. Temperature-induced regulation of RpoS by a small RNA in *Borrelia burgdorferi*. Mol Microbiol. 2007; 64:1075–1089. [PubMed: 17501929]

Ouyang Z, Deka RK, Norgard MV. BosR (BB0647) controls the RpoN-RpoS regulatory pathway and virulence expression in *Borrelia burgdorferi* by a novel DNA-binding mechanism. PLoS Pathog. 2011; 7:e1001272. [PubMed: 21347346]

Ouyang Z, Narasimhan S, Neelakanta G, Kumar M, Pal U, Fikrig E, et al. Activation of the RpoN-RpoS regulatory pathway during the enzootic life cycle of *Borrelia burgdorferi*. BMC Microbiol. 2012; 12:44. [PubMed: 22443136]

Pal U, Yang X, Chen M, Bockenstedt LK, Anderson JF, Flavell RA, et al. OspC facilitates *Borrelia burgdorferi* invasion of *Ixodes scapularis* salivary glands. J Clin Invest. 2004; 113:220–230. [PubMed: 14722614]

Pappas CJ, Iyer R, Petzke MM, Caimano MJ, Radolf JD, Schwartz I. *Borrelia burgdorferi* requires glycerol for maximum fitness during the tick phase of the enzootic cycle. PLoS Pathog. 2011; 7:e1002102. [PubMed: 21750672]

Pennetier C, Dominguez-Ramirez L, Plumbridge J. Different regions of Mlc and NagC, homologous transcriptional repressors controlling expression of the glucose and N-acetylglucosamine phosphotransferase systems in *Escherichia coli*, are required for inducer signal recognition. Mol Microbiol. 2008; 67:364–377. [PubMed: 18067539]

Plumbridge J. Co-ordinated regulation of amino sugar biosynthesis and degradation: the NagC repressor acts as both an activator and a repressor for the transcription of the *glmUS* operon and requires two separated NagC binding sites. EMBO J. 1995; 14:3958–3965. [PubMed: 7545108]

Plumbridge J. How to achieve constitutive expression of a gene within an inducible operon: the example of the *nagC* gene of *Escherichia coli*. J Bacteriol. 1996; 178:2629–2636. [PubMed: 8626331]

Plumbridge J. Regulation of PTS gene expression by the homologous transcriptional regulators, Mlc and NagC, in *Escherichia coli* (or how two similar repressors can behave differently). J Mol Microbiol Biotechnol. 2001; 3:371–380. [PubMed: 11361067]

Plumbridge J. Regulation of gene expression in the PTS in *Escherichia coli:* the role and interactions of Mlc. Curr Opin Microbiol. 2002; 5:187–193. [PubMed: 11934616]

Plumbridge J, Pellegrini O. Expression of the chitobiose operon of *Escherichia coli* is regulated by three transcription factors: NagC, ChbR and CAP. Mol Microbiol. 2004; 52:437–449. [PubMed: 15066032]

Plumbridge JA. Repression and induction of the nag regulon of *Escherichia coli* K-12: the roles of *nagC* and *nagA* in maintenance of the uninduced state. Mol Microbiol. 1991; 5:2053–2062. [PubMed: 1766379]

Poncet S, Milohanic E, Maze A, Nait Abdallah J, Ake F, Larribe M, et al. Correlations between carbon metabolism and virulence in bacteria. Contrib Microbiol. 2009; 16:88–102. [PubMed: 19494580]

Postma PW, Lengeler JW, Jacobson GR. Phosphoenolpyruvate:carbohydrate phosphotransferase systems of bacteria. Microbiol Rev. 1993; 57:543–594. [PubMed: 8246840]

Radolf JD, Caimano MJ, Stevenson B, Hu LT. Of ticks, mice and men: understanding the dual-host lifestyle of Lyme disease spirochaetes. Nat Rev Microbiol. 2012; 10:87–99. [PubMed: 22230951]

Raju BV, Esteve-Gassent MD, Karna SL, Miller CL, Van Laar TA, Seshu J. Oligopeptide permease A5 modulates vertebrate host-specific adaptation of *Borrelia burgdorferi*. Infect Immun. 2011; 79:3407–3420. [PubMed: 21628523]

Rhodes RG, Atoyan JA, Nelson DR. The chitobiose transporter, *chbC*, is required for chitin utilization in *Borrelia burgdorferi*. BMC Microbiol. 2010; 10:21. [PubMed: 20102636]

Rhodes RG, Coy W, Nelson DR. Chitobiose utilization in *Borrelia burgdorferi* is dually regulated by RpoD and RpoS. BMC Microbiol. 2009; 9:108. [PubMed: 19473539]

Rogers EA, Terekhova D, Zhang HM, Hovis KM, Schwartz I, Marconi RT. Rrp1, a cyclic-di-GMP-producing response regulator, is an important regulator of *Borrelia burgdorferi* core cellular functions. Mol Microbiol. 2009; 71:1551–1573. [PubMed: 19210621]

Samuels DS. Electrotransformation of the spirochete *Borrelia burgdorferi*. Methods Mol Biol. 1995; 47:253–259. [PubMed: 7550741]

Samuels DS. Gene regulation in *Borrelia burgdorferi*. Annu Rev Microbiol. 2011; 65:479–499. [PubMed: 21801026]

Sanjuan E, Esteve-Gassent MD, Maruskova M, Seshu J. Overexpression of CsrA (BB0184) alters the morphology and antigen profiles of *Borrelia burgdorferi*. Infect Immun. 2009; 77:5149–5162. [PubMed: 19737901]

Schiefner A, Gerber K, Seitz S, Welte W, Diederichs K, Boos W. The crystal structure of Mlc, a global regulator of sugar metabolism in *Escherichia coli*. J Biol Chem. 2005; 280:29073–29079. [PubMed: 15929984]

Schneider CA, Rasband WS, Eliceiri KW. NIH Image to ImageJ: 25 years of image analysis. Nat Methods. 2012; 9:671–675. [PubMed: 22930834]

Shin D, Lim S, Seok YJ, Ryu S. Heat shock RNA polymerase (E sigma(32)) is involved in the transcription of *mlc* and crucial for induction of the Mlc regulon by glucose in *Escherichia coli*. J Biol Chem. 2001; 276:25871–25875. [PubMed: 11340070]

Smyth GK. Linear models and empirical bayes methods for assessing differential expression in microarray experiments. Stat Appl Genet Mol Biol. 2004; 3 Article3.

Sohanpal BK, Friar S, Roobol J, Plumbridge JA, Blomfield IC. Multiple co-regulatory elements and IHF are necessary for the control of *fimB* expression in response to sialic acid and N-acetylglucosamine in *Escherichia coli* K-12. Mol Microbiol. 2007; 63:1223–1236. [PubMed: 17238917]

Steere AC. Lyme borreliosis in 2005, 30 years after initial observations in Lyme Connecticut. Wien Klin Wochenschr. 2006; 118:625–633. [PubMed: 17160599]

Stevenson B, Zuckert WR, Akins DR. Repetition, conservation, and variation: the multiple cp32 plasmids of *Borrelia* species. J Mol Microbiol Biotechnol. 2000; 2:411–422. [PubMed: 11075913]

Strother KO, Broadwater A, De Silva A. Plasmid requirements for infection of ticks by *Borrelia burgdorferi*. Vector Borne Zoonotic Dis. 2005; 5:237–245. [PubMed: 16187892]

Sultan SZ, Pitzer JE, Miller MR, Motaleb MA. Analysis of a *Borrelia burgdorferi* phosphodiesterase demonstrates a role for cyclic-di-guanosine monophosphate in motility and virulence. Mol Microbiol. 2010; 77:128–142. [PubMed: 20444101]

Sze CW, Li C. Inactivation of *bb0184*, which encodes carbon storage regulator A, represses the infectivity of *Borrelia burgdorferi*. Infect Immun. 2011; 79:1270–1279. [PubMed: 21173314]

Sze CW, Morado DR, Liu J, Charon NW, Xu H, Li C. Carbon storage regulator A (CsrA(Bb)) is a repressor of *Borrelia burgdorferi* flagellin protein FlaB. Mol Microbiol. 2011; 82:851–864. [PubMed: 21999436]

Tanaka Y, Kimata K, Aiba H. A novel regulatory role of glucose transporter of *Escherichia coli:* membrane sequestration of a global repressor Mlc. EMBO J. 2000; 19:5344–5352. [PubMed: 11032802]

Tilly K, Elias AF, Errett J, Fischer E, Iyer R, Schwartz I, et al. Genetics and regulation of chitobiose utilization in *Borrelia burgdorferi*. J Bacteriol. 2001; 183:5544–5553. [PubMed: 11544216]

Tilly K, Grimm D, Bueschel DM, Krum JG, Rosa P. Infectious cycle analysis of a *Borrelia burgdorferi* mutant defective in transport of chitobiose, a tick cuticle component. Vector Borne Zoonotic Dis. 2004; 4:159–168. [PubMed: 15228817]

Titgemeyer F, Reizer J, Reizer A, Saier MH Jr. Evolutionary relationships between sugar kinases and transcriptional repressors in bacteria. Microbiology. 1994; 140(Pt 9):2349–2354. [PubMed: 7952186]

Tokarz R, Anderton JM, Katona LI, Benach JL. Combined effects of blood and temperature shift on *Borrelia burgdorferi* gene expression as determined by whole genome DNA array. Infect Immun. 2004; 72:5419–5432. [PubMed: 15322040]

Van Laar TA, Lin YH, Miller CL, Karna SL, Chambers JP, Seshu J. Effect of Levels of Acetate on the Mevalonate Pathway of *Borrelia burgdorferi*. PLoS One. 2012; 7:e38171. [PubMed: 22675445]

von Lackum K, Stevenson B. Carbohydrate utilization by the Lyme borreliosis spirochete, *Borrelia burgdorferi*. FEMS Microbiol Lett. 2005; 243:173–179. [PubMed: 15668016]

Xu Y, Bruno JF, Luft BJ. Profiling the humoral immune response to *Borrelia burgdorferi* infection with protein microarrays. Microb Pathog. 2008; 45:403–407. [PubMed: 18976702]

Yang XF, Alani SM, Norgard MV. The response regulator Rrp2 is essential for the expression of major membrane lipoproteins in *Borrelia burgdorferi*. Proc Natl Acad Sci U S A. 2003; 100:11001–11006. [PubMed: 12949258]

A

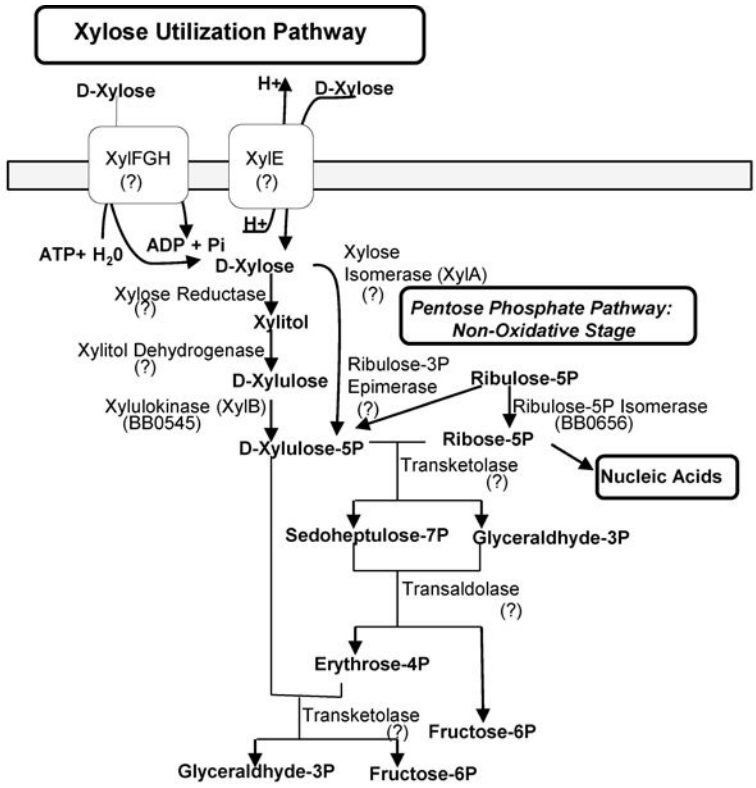

B

ROKs	Species		Helix 1									Turn			Helix 2											
NagC	*E. coli*	33	I	S	R	I	Q	I	A	E	Q	S	Q	L	A	P	A	S	V	T	K	I	T	R	Q	L	56
Mlc	*E. coli*	31	V	S	R	I	D	L	S	R	L	A	Q	L	A	P	A	S	I	T	K	I	V	R	E	M	54
XylR	*B. subtilis*	27	I	S	R	A	K	L	S	E	M	T	G	L	N	K	S	T	V	S	S	Q	V	N	T	L	50
XylR1	*B. burgdorferi*	28	Y	S	R	T	D	L	A	R	K	L	S	L	T	N	A	A	V	T	I	L	T	N	Q	M	51

♦ Single, fully conserved residue
† Conservation of strong groups
• Conservation of weak groups

Fig. 1.

Analysis of xylose utilization of *B. burgdorferi* and ROK DNA-binding domains. BLAST analysis in conjunction with the borrelial genome annotations (Fraser *et al.*, 1997) demonstrated xylulokinase (BB0545) as the only enzyme for xylose utilization in *B. burgdorferi* suggesting ORFs annotated as xylose operon regulatory proteins (XylR1 and XylR2) are misannotated and have alternative functions **(A)**. Comparison of ROK DNA-binding motifs. Alignment of the HTH motifs in the N-terminal regions of NagC and Mlc from *E. coli*, XylR repressor from *Bacillus subtilis*, and XylR1 from *B. burgdorferi.* The locations of the motifs relative to the N-terminus of the proteins are given. Conservation stringency of residues is depicted using symbols below **(B)**.

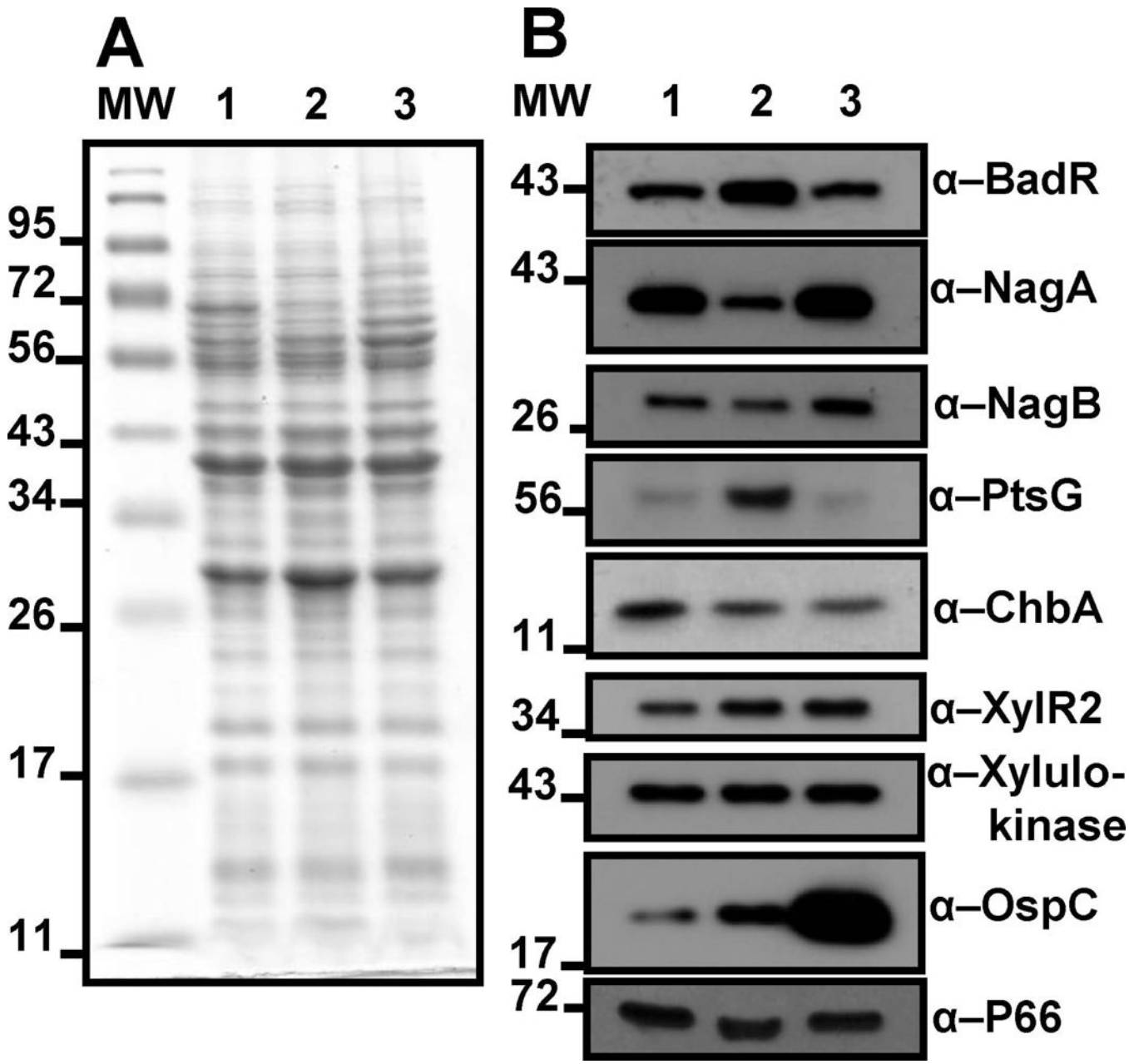

Fig. 2.

Immunoblot analysis determines regulatory contributions of BadR. Coomassie blue stained SDS-PAGE of *B. burgdorferi* B31-A3 lysates grown under host-mimicking conditions **(A)**. Immunoblot analysis using depicted antibodies **(B)**. Lanes: MW: molecular weight marker, 1: grown at pH7.6/32°C; 2: grown at pH 7.6/23°C (mimicking unfed-tick); 3: grown at pH 6.8/37°C (mimicking fed-tick).

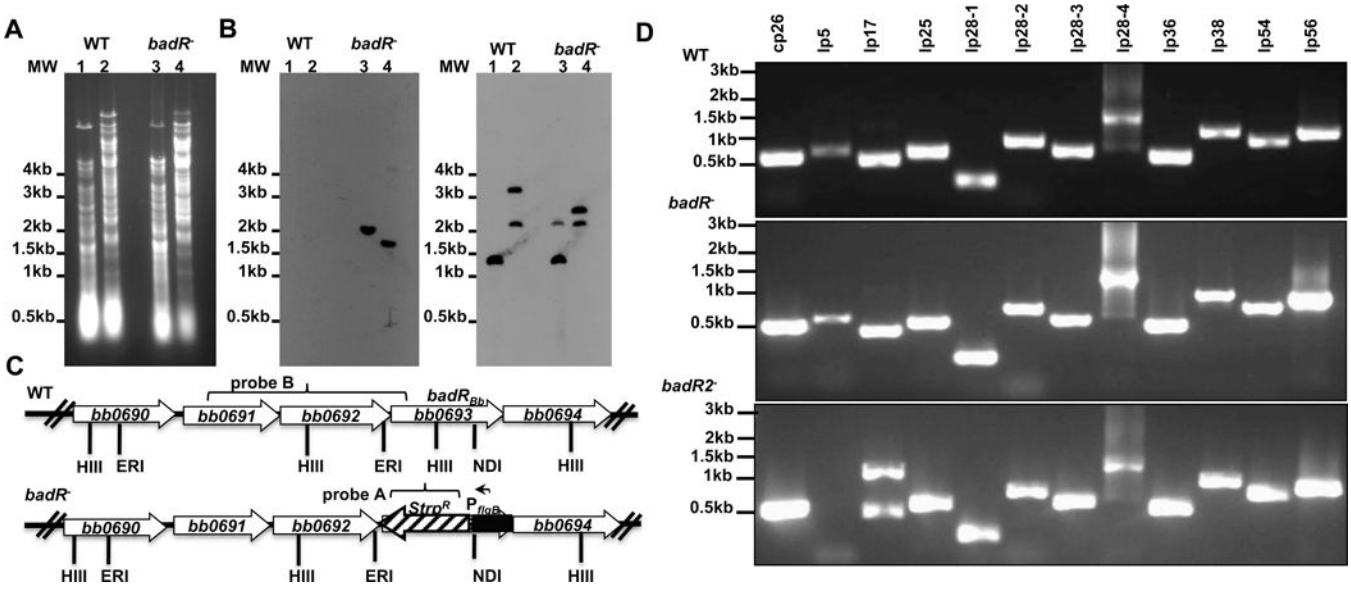

Fig. 3.

Genetic analyses of *badR*-deficient *B. burgdorferi* strains. Total genomic DNA from parental B31-A3 (WT) and *badR*-deficient strain (*badR*$^{-}$) was digested with HindIII (lanes 1 and 3) or EcoRI and NdeI (lanes 2 and 4), separated on a 1% agarose gel, and transferred to nylon membranes **(A, B, C)**. Membranes were hybridized with PCR amplified probes corresponding to the *aadA* gene (Str^{R} marker) **(B)** or to a region upstream of the *badR* gene **(C)**. Schematic representation of the *badR* region of the chromosome for both WT and *badR*$^{-}$. Probes used are indicated with brackets. HIII-HindIII, ERI-EcoRI, ND1-NdeI **(D)**. PCR confirmation to assess plasmid profile was performed on parental and *badR*-deficient strains. Strains and molecular weight (in base pairs) are indicated on the left **(E)**.

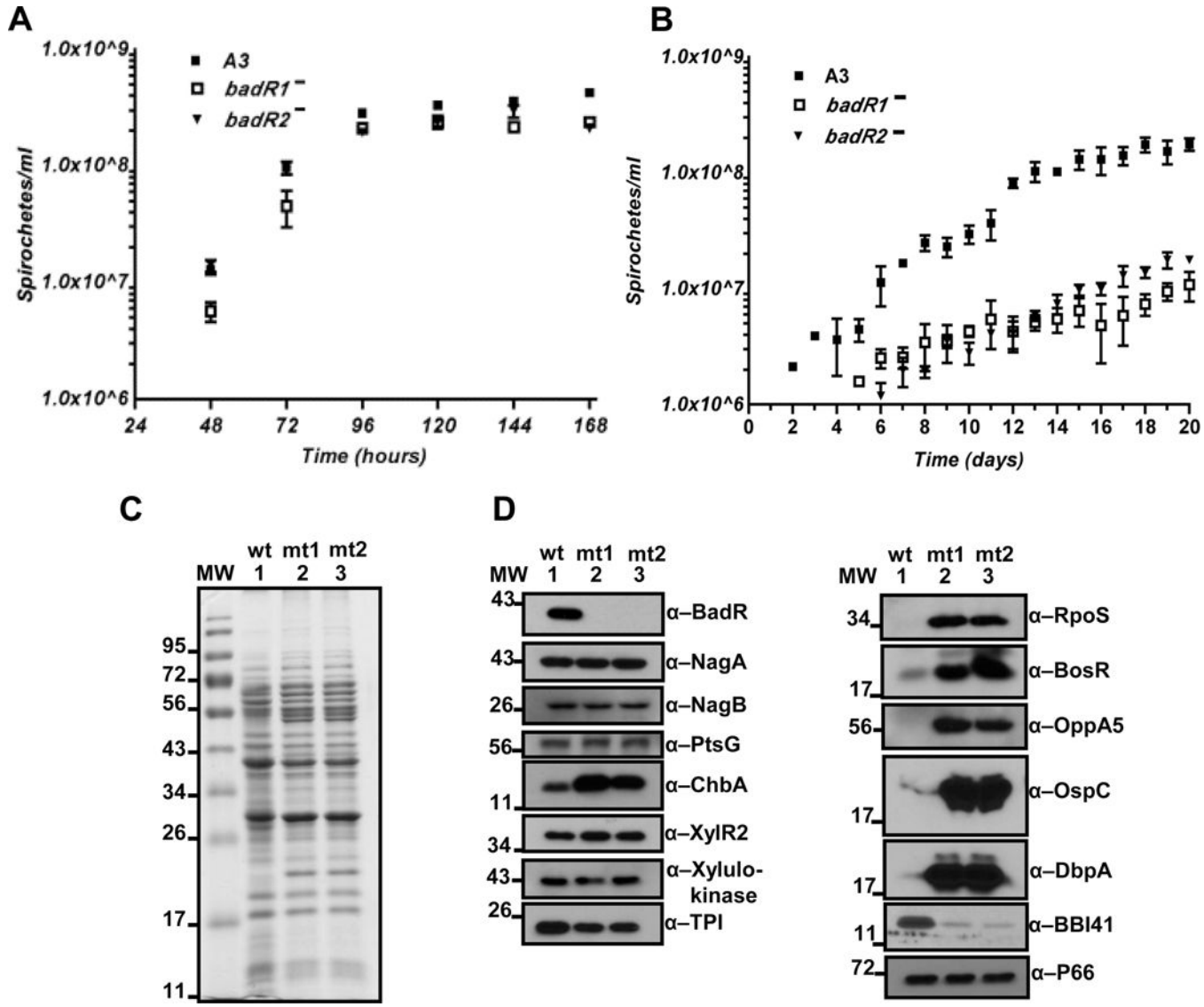

Fig. 4.

Growth analysis and protein profile of *badR*-deficient strains. Growth analysis of WT and *badR*-deficient strains grown under laboratory (pH7.6/32°C) **(A)** and unfed-tick (pH7.6/23°C) **(B)** conditions. Bacteria were diluted from stationary phase (1×10^8 bacteria ml^{-1}), seeded at 5×10^5 bacteria ml^{-1}, and enumerated every 24 hours using dark field microscopy. The cultures were grown in triplicate, with three independent trials. Error bars indicate standard error. Levels of significance were determined using two-way ANOVA with α=95% and there were statistical differences in growth in the *badR*-deficient strains from day 11 on with a $P<0.01$ **(A, B)**. Protein profile of *badR*-deficient *B. burgdorferi*. Coomassie blue stained SDS-PAGE of *B. burgdorferi* lysates from WT (B31-A3) and *badR*-deficient strains grown under laboratory growth conditions (pH7.6/32°C) **(C)**. Immunoblot analysis using depicted antibodies. Lanes: MW: molecular weight marker in kDa; 1: parental B31-A3 (wt); 2: *badR*⁻ (mt1); 3: *badR2*⁻ (mt2) **(D)**.

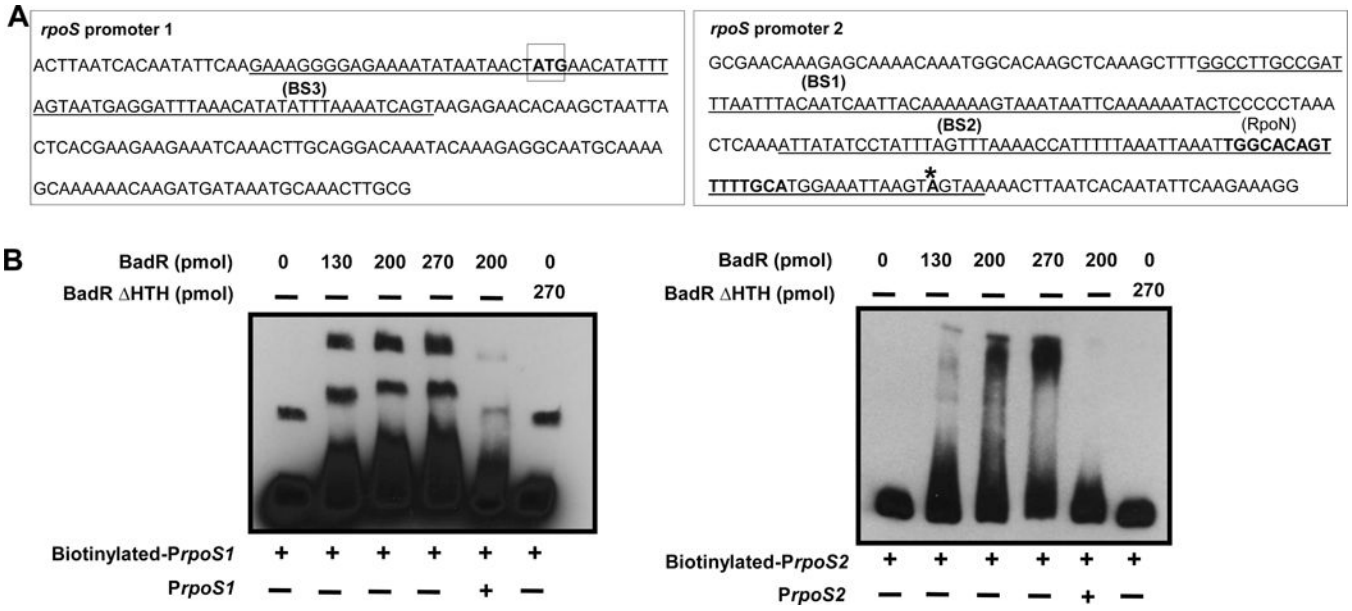

Fig. 5.

BadR binds *rpoS* promoters. Schematic diagram illustrating the two regions upstream of *rpoS* used for the EMSAs. RpoS 1 promoter (P*rpoS* $1_{(813088\text{-}813282)}$) includes the RpoS start codon (boxed) and BosR binding site 3 (BS3 -Underlined). RpoS2 promoter (P*rpoS* $2_{(813258\text{-}813471)}$) includes the RpoN binding site (bold), both the BosR binding sites 1 and 2 (BS1, BS2 -Underlined), and the *rpoS* transcriptional start site (bolded with asterisk) **(A)**. 5′ biotin-labeled promoters (2 nmols) were mixed with various amounts of purified $BadR_{(734081\text{-}735289)}$ (130, 200, 270 pmols) in a 20μl binding reaction. Some reactions were incubated with unlabeled promoters (200-fold molar excess) for competition reactions or a N′ terminal HTH deficient $BadR_{(734225\text{-}735289)}$ (BadR Δ HTH) **(B)**. The binding reactions were incubated at room temperature for 20 minutes, run on a 6% polyacrylamide gel, and transferred onto a positively charged Nylon membrane. After transfer the membrane was cross-linked by UV irradiation, blocked, incubated with streptavidin-horseradish peroxidase conjugate and luminol enhancer substrate solution allowed visualization of labeled DNA by exposure to X-ray film.

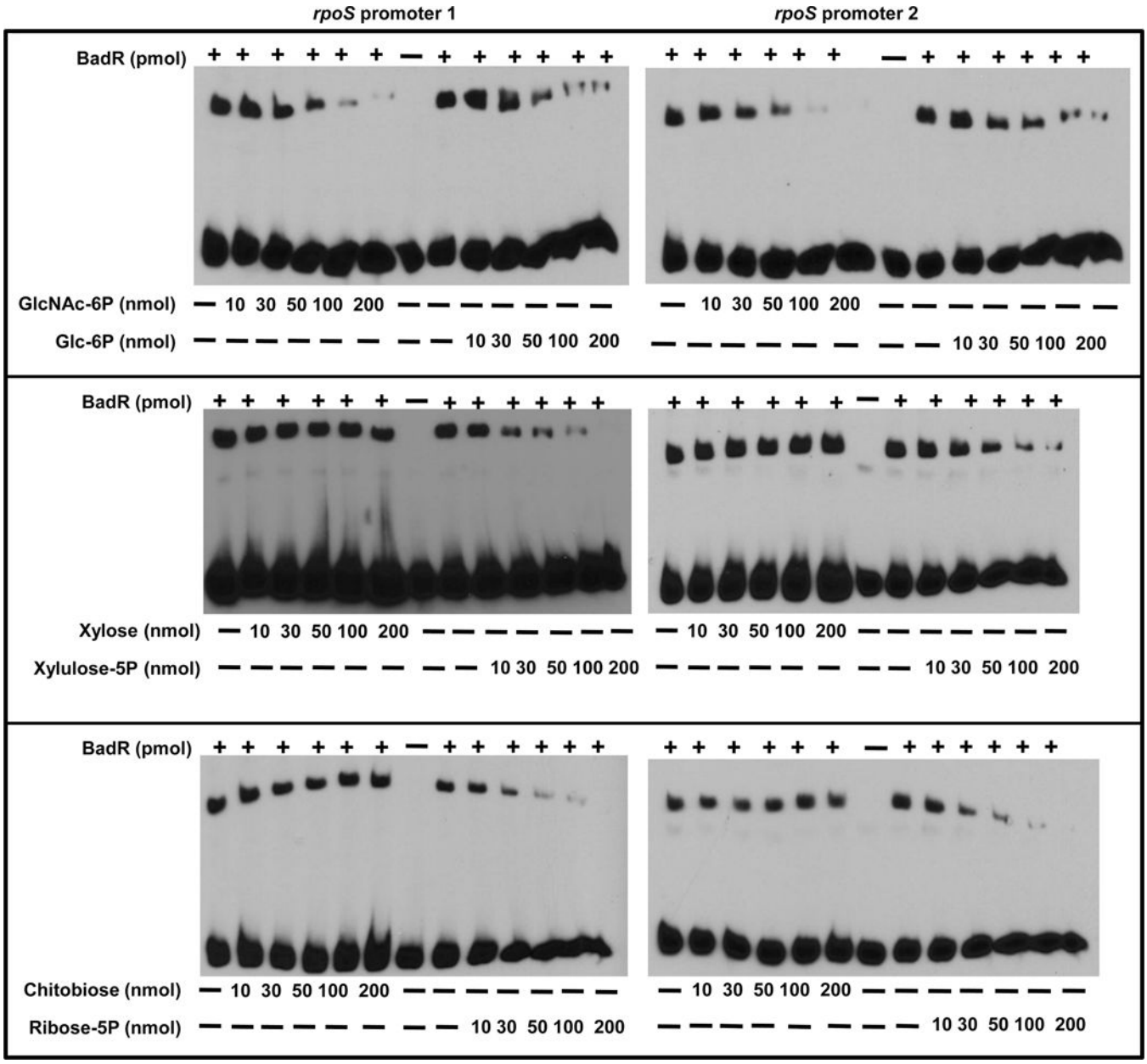

Fig. 6.

Phosphorylated sugars alleviate BadR binding to *rpoS* promoters. Two nmols of 5′ biotinylated *rpoS* promoters (P*rpoS* 1**(A)**, P*rpoS* 2 **(B)**) were mixed with 130 pmols of WT BadR. The binding reactions were performed in the absence or presence of various sugars (GlcNAc-6P, glucose-6P (Glc-6P), xylulose-5P, ribose-5P, xylose, or chitobiose). Binding reactions with various sugar concentrations (10, 30, 50,100, or 200mM) determined the influence of each sugar on BadR binding to the *rpoS* promoters.

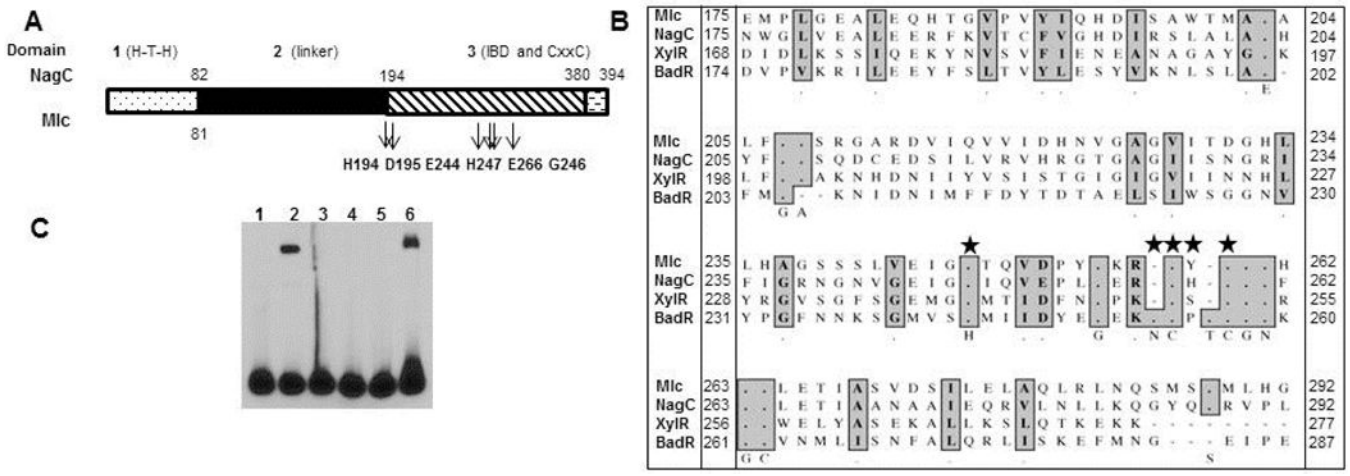

Fig. 7.

Characterization of BadR: Site-directed mutations and domain-deficient BadRs. Schematic representation of BadR domains **(A)** and comparisons of residues in ROK inducer-binding domains (IBD). Mutated residues are indicated (star) **(B)**. 5′ biotinylated *rpoS* promoter 1 (2 nmols) was incubated with WT or mutant BadR proteins (130pmols) as previously described. Lanes: binding reaction absent of BadR (1), WT $BadR_{(734081-735289)}$ (2), BadR Δ HTH ($BadR_{(734225-735289)}$) (3), BadR deficient of inducer binding domain $BadR_{(734081-734659)}$ (BadRΔIBD) (4), BadR with a site directed mutation in the equivalent residue of the ROK conserved residue, H247, (H243A) (5), BadR with site-directed mutations in the putative ROK CxxC metal binding/dimerization residues, (C254A/C257A) (6), BadR with site directed mutations in unique residues in BadR's putative inducer binding domain (N253A/P255A) (7) **(C)**.

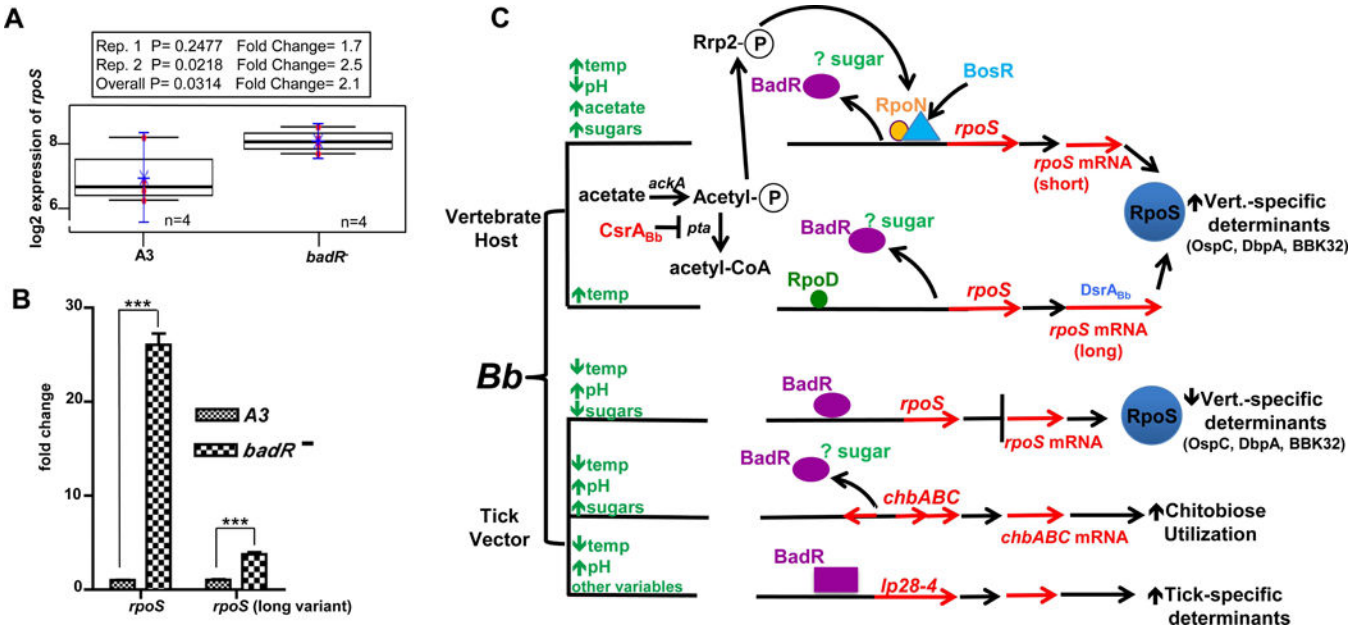

Fig. 8.

BadR represses *rpoS* to regulate host-specific adaptation in *B. burgdorferi.* The *rpoS* gene is upregulated in a *badR*-deficient *B. burgdorferi strain.* Log2 fold change of *rpoS* derived from two microarrays from (pH7.6/32°C) grown cultures. P values from pooled (overall) and individual arrays (Rep.1, Rep.2) are indicated using n=4 for both A3 (WT) and *badR*$^{-}$ **(A)**. Quantitative RT-PCR fold changes of *rpoS* are indicated with $P \leq 0.01$. Error bars indicate s.e.m. **(B)**. Predicted BadR regulatory network. Many activators of *rpoS* have been identified (e.g. $DsrA_{Bb}$, BosR, RpoN, RpoD, $CsrA_{Bb}$). Our study is the first to demonstrate BadR as a repressor of *rpoS* and thus may facilitate the spirochete's transition back into ticks. A model for BadR regulation entails the following: 1.) BadR binds upstream of *rpoS* to repress *rpoS* in unfed ticks; 2.) Since ROK regulators are nutrient-responsive, BadR regulation may be modulated directly or indirectly by nutrient inducers; 3.) Nutrient surges from the blood meal may provide the inducer to allow BadR's derepression of *rpoS*; and 4.) BadR regulates chitobiose utilization genes and may activate genes to enhance the spirochetes maintenance in ticks (lp28-4 genes). square= activation, oval=repression by BadR, respectively **(C)**.

Mol Microbiol. Author manuscript; available in PMC 2016 April 12.

Table 1

Genes differentially expressed in the *badR*-deficient strain.

Gene ID	Function (Annotation)	Replicon	$FC_{Overall}$	$95\%CI_{Low}$	$95\%CI_{High}$	$P_{Overall}$	FDR
	Up-regulated in *badR*$^{-}$						
BBB19	outer surface protein C (*ospC*)	cp26	75.21	54.07	104.61	2.84E-08	4.74E-06
BBA36	lipoprotein	lp54	64.27	52.31	78.97	6.62E-10	1.02E-06
BBA37	hypothetical protein	lp54	61.94	48.21	79.58	3.93E-09	1.53E-06
BBA65	hypothetical protein	lp54	54.41	39.08	75.74	5.66E-08	6.69E-06
BBA73	antigen, P35, putative	lp54	36.52	27.23	48.96	4.97E-08	6.37E-06
BBD07	hypothetical protein	lp17	33.11	13.25	82.78	5.37E-04	8.42E-03
BBA25	decorin binding protein B (*dbpB*)	lp54	32.85	17.48	61.71	3.50E-05	1.15E-03
BBA72	hypothetical protein	lp54	30.38	20.93	44.10	5.91E-07	3.63E-05
BBB05	PTS system, chitobiose-specific IIA component (*chbC*)	cp26	24.06	17.73	32.64	1.99E-07	1.60E-05
BBJ23	hypothetical protein	lp38	22.83	13.95	37.36	1.19E-05	4.59E-04
BBA66	antigen, P35, putative	lp54	19.76	14.63	26.69	3.00E-07	2.03E-05
BBA07	chpAI protein, putative	lp54	17.67	12.25	25.49	2.15E-06	1.00E-04
BBA71	hypothetical protein	lp54	17.48	13.52	22.59	1.12E-07	1.23E-05
BBH41	hypothetical protein	lp28-3	17.23	10.13	29.29	4.48E-05	1.41E-03
BBB06	PTS system, chitobiose-specific IIB component (*chbA*)	cp26	17.07	12.03	24.23	1.64E-06	8.19E-05
BBA05	antigen, S1	lp54	16.00	9.34	27.42	6.13E-05	1.66E-03
BB0844	hypothetical protein	chromosome	15.82	9.65	25.91	3.25E-05	1.11E-03
BBA33	hypothetical protein	lp54	13.89	10.18	18.95	1.14E-06	6.49E-05
BBP27	rev protein	cp32-1	12.50	10.33	15.14	2.65E-08	4.74E-06
BBQ37	hypothetical protein	lp56	10.48	6.48	16.95	9.13E-05	2.24E-03
BBM29	hypothetical protein	cp32-6	10.26	6.41	16.44	8.37E-05	2.21E-03
BBP28	lipoprotein	cp32-1	9.98	7.51	13.28	1.70E-06	8.19E-05
BBM38	ErpK	cp32-6	8.91	6.56	12.10	4.65E-06	1.99E-04
BBB07	outer surface protein, putative	cp26	8.62	7.30	10.17	3.08E-08	4.74E-06
BBO39	ErpL	cp32-7	8.50	5.66	12.77	5.17E-05	1.53E-03
BBA34	oligopeptide ABC transporter, periplasmic oligopeptide-binding protein (*oppAV*)	lp54	7.83	5.10	12.02	1.04E-04	2.43E-03
BBA24	decorin binding protein A (*dbpA*)	lp54	7.65	6.28	9.32	2.18E-07	1.60E-05

Gene ID	Function (Annotation)	Replicon	$FC_{Overall}$	$95\%CI_{Low}$	$95\%CI_{High}$	$P_{Overall}$	FDR
	Up-regulated in *badR*$^{-}$						
BBK32	immunogenic protein P35	lp36	7.36	4.57	11.86	2.82E-04	5.33E-03
BBA04	antigen, S2	lp54	7.06	5.54	8.99	1.68E-06	8.19E-05
BBB04	PTS system, chitobiose-specific IIC component (*chbB*)	cp26	6.71	5.34	8.44	1.33E-06	7.04E-05
BBJ01	hypothetical protein	lp38	5.66	4.60	6.96	1.24E-06	6.81E-05
BBI42	hypothetical protein	lp28-4	4.96	3.67	6.71	4.87E-05	1.47E-03
BBS41	ErpG	cp32-3	4.84	3.79	6.18	1.04E-05	4.11E-04
BBQ05	antigen, P35, putative	lp56	4.74	3.36	6.69	1.65E-04	3.58E-03
BBF01	erpD protein, putative	lp28-1	4.56	3.34	6.23	9.18E-05	2.24E-03
BBE31	antigen, P35, putative	lp-25	4.53	2.98	6.89	7.91E-04	1.16E-02
BBQ03	outer membrane protein, putative	lp56	4.50	3.38	6.00	5.33E-05	1.55E-03
BBK12	hypothetical protein	lp36	4.43	2.46	7.96	6.81E-03	4.99E-02
BBK03	hypothetical protein	lp36	4.14	2.85	6.01	5.38E-04	8.42E-03
BBJ48	hypothetical protein	lp38	4.12	2.73	6.22	1.11E-03	1.52E-02
BBK53	outer membrane protein	lp36	4.07	2.97	5.59	1.88E-04	3.80E-03
BBK07	hypothetical protein	lp36	4.00	2.94	5.44	1.69E-04	3.58E-03
BBA64	antigen, P35	lp54	3.95	2.54	6.14	2.06E-03	2.33E-02
BBQ89	hypothetical protein	lp56	3.94	3.11	5.00	2.57E-05	9.40E-04
BBR28	lipoprotein	cp32-4	3.71	2.64	5.21	5.04E-04	8.08E-03
BBD24	hypothetical protein	lp17	3.69	2.42	5.60	2.04E-03	2.33E-02
BBK52	protein p23	lp36	3.56	2.35	5.41	2.36E-03	2.42E-02
BBM39	hypothetical protein	cp32-6	3.40	2.74	4.22	2.83E-05	9.90E-04
BBQ38	hypothetical protein	lp56	3.19	1.94	5.25	1.06E-02	6.65E-02
BBP03	hypothetical protein	cp32-1	3.17	2.54	3.96	5.72E-05	1.63E-03
BBJ24	hypothetical protein	lp38	3.16	1.91	5.21	1.14E-02	6.92E-02
BBA57	hypothetical protein	lp54	3.14	2.53	3.90	4.84E-05	1.47E-03
BBA06	hypothetical protein	lp54	3.04	2.07	4.45	3.08E-03	2.93E-02
BBA01	hypothetical protein	lp54	2.92	2.15	3.97	9.83E-04	1.37E-02
BBL30	hypothetical protein	cp32-8	2.86	1.84	4.44	9.66E-03	6.27E-02
BBB10	hypothetical protein	cp26	2.85	1.73	4.70	1.77E-02	8.98E-02
BBJ46	hypothetical protein	lp38	2.79	1.99	3.90	2.34E-03	2.42E-02

Mol Microbiol. Author manuscript; available in PMC 2016 April 12.

Gene ID	Function (Annotation)	Replicon	$FC_{Overall}$	$95\%CI_{Low}$	$95\%CI_{High}$	$P_{Overall}$	FDR
	Up-regulated in *badR*$^{-}$						
BBR29	hypothetical protein	cp32-4	2.78	1.94	3.98	3.55E-03	3.19E-02
BBP38	ErpA	cp32-1	2.78	1.87	4.13	6.33E-03	4.77E-02
BBO40	ErpM	cp32-7	2.76	1.68	4.53	2.03E-02	9.65E-02
BBJ03	hypothetical protein	lp38	2.74	1.55	4.84	3.71E-02	1.39E-01
BBO02	hypothetical protein	cp32-7	2.72	2.30	3.22	2.02E-05	7.59E-04
BBS31	hypothetical protein	cp32-3	2.69	1.77	4.10	1.01E-02	6.41E-02
BBQ47	ErpX	lp56	2.69	1.81	4.00	7.54E-03	5.34E-02
BBS42	BapA	cp32-3	2.66	1.86	3.82	4.52E-03	3.78E-02
BBQ82	hypothetical protein	lp56	2.65	2.07	3.41	4.55E-04	7.45E-03
BBR40	ErpH	cp32-4	2.62	1.91	3.59	2.34E-03	2.42E-02
BBP29	hypothetical protein	cp32-1	2.60	1.73	3.93	1.07E-02	6.65E-02
BBJ02	hypothetical protein	lp38	2.59	2.09	3.20	1.77E-04	3.68E-03
BB0845	hypothetical protein	chromosome	2.55	1.69	3.86	1.20E-02	7.11E-02
BBR31	hypothetical protein	cp32-4	2.54	1.57	4.13	2.62E-02	1.14E-01
BBA32	hypothetical protein	lp54	2.54	1.91	3.36	1.45E-03	1.82E-02
BBP02	hypothetical protein	cp32-1	2.51	2.10	2.99	5.82E-05	1.63E-03
BBO29	hypothetical protein	cp32-7	2.49	1.63	3.81	1.62E-02	8.48E-02
BBJ25	hypothetical protein	lp38	2.47	1.89	3.24	1.29E-03	1.66E-02
BBK50	immunogenic protein P37	lp36	2.44	1.48	4.02	3.65E-02	1.39E-01
BBP35	BppA	cp32-1	2.42	1.84	3.18	1.59E-03	1.96E-02
BBQ52	hypothetical protein	lp56	2.42	2.04	2.87	6.14E-05	1.66E-03
BBP01	hypothetical protein	cp32-1	2.40	1.96	2.94	2.27E-04	4.53E-03
BBJ47	hypothetical protein	lp38	2.38	1.72	3.29	5.11E-03	4.16E-02
BBS38	BppA	cp32-3	2.38	1.81	3.12	1.83E-03	2.16E-02
BBM02	hypothetical protein	cp32-6	2.37	1.95	2.88	1.86E-04	3.80E-03
BBS02	hypothetical protein	cp32-3	2.36	1.98	2.82	9.46E-05	2.24E-03
BBA23	hypothetical protein	lp54	2.36	1.65	3.37	9.13E-03	6.02E-02
BBM01	antigen, P35, putative	cp32-6	2.35	1.95	2.84	1.55E-04	3.45E-03
BBR01	antigen, P35, putative	cp32-4	2.35	1.95	2.83	1.39E-04	3.15E-03
BBM35	BppA	cp32-6	2.32	1.81	2.99	1.27E-03	1.66E-02

Mol Microbiol. Author manuscript; available in PMC 2016 April 12.

Gene ID	Function (Annotation)	Replicon	$FC_{Overall}$	$95\%CI_{Low}$	$95\%CI_{High}$	$P_{Overall}$	FDR
	Up-regulated in *badR*$^{-}$						
BBN38	ErpP	cp32-9	2.32	1.77	3.05	2.08E-03	2.33E-02
BBE04	hypothetical protein	lp-25	2.31	1.53	3.51	2.12E-02	9.94E-02
BBS01	hypothetical protein	cp32-3	2.29	1.84	2.85	5.48E-04	8.44E-03
BBA35	hypothetical protein	lp54	2.27	1.78	2.89	1.24E-03	1.64E-02
BBK48	immunogenic protein P37, putative	lp36	2.26	1.56	3.26	1.41E-02	7.94E-02
BBP10	hypothetical protein	cp32-1	2.25	1.84	2.75	3.89E-04	6.65E-03
BBQ88	hypothetical protein	lp56	2.23	1.47	3.39	2.59E-02	1.14E-01
BBJ19	hypothetical protein	lp38	2.23	1.71	2.90	2.35E-03	2.42E-02
BBG22	hypothetical protein	lp28-2	2.23	1.73	2.87	1.84E-03	2.16E-02
BBH36	hypothetical protein	lp28-3	2.20	1.72	2.82	1.76E-03	2.12E-02
BBQ43	BppA	lp56	2.20	1.80	2.69	4.47E-04	7.40E-03
BBM37	BppC	cp32-6	2.20	1.73	2.78	1.35E-03	1.72E-02
BBR10	hypothetical protein	cp32-4	2.20	1.75	2.75	9.81E-04	1.37E-02
BBO30	hypothetical protein	cp32-7	2.19	1.72	2.80	1.69E-03	2.06E-02
BBO36	BppA	cp32-7	2.19	1.80	2.65	3.63E-04	6.28E-03
BBK11	hypothetical protein	lp36	2.18	1.80	2.63	3.24E-04	5.87E-03
BBN10	hypothetical protein	cp32-9	2.17	1.77	2.67	5.42E-04	8.42E-03
BBQ06	hypothetical protein	lp56	2.16	1.57	2.98	9.18E-03	6.03E-02
BBQ10	hypothetical protein	lp56	2.16	1.79	2.60	3.02E-04	5.53E-03
BBJ26	ABC transporter, ATP-binding protein	lp38	2.16	1.55	3.00	1.07E-02	6.65E-02
BBQ45	BppC	lp56	2.15	1.63	2.83	4.17E-03	3.59E-02
BBL36	BppA	cp32-8	2.14	1.77	2.58	3.52E-04	6.23E-03
BBN30	hypothetical protein	cp32-9	2.13	1.63	2.77	3.56E-03	3.19E-02
BBO01	hypothetical protein	cp32-7	2.12	1.78	2.53	2.46E-04	4.79E-03
BBQ29	hypothetical protein	lp56	2.11	1.64	2.71	2.87E-03	2.80E-02
BBH02	hypothetical protein	lp28-3	2.10	1.49	2.95	1.49E-02	8.11E-02
BBA76	thymidylate synthase	lp54	2.07	1.56	2.73	6.00E-03	4.58E-02
BBN35	BppA	cp32-9	2.07	1.63	2.62	2.36E-03	2.42E-02
BB0771	RNA polymerase sigma factor (*rpoS*)	chromosome	2.06	1.39	3.05	3.14E-02	1.28E-01
BBS04	hypothetical protein	cp32-3	2.06	1.71	2.48	4.94E-04	7.99E-03

Mol Microbiol. Author manuscript; available in PMC 2016 April 12.

Gene ID	Function (Annotation)	Replicon	$FC_{Overall}$	$95\%CI_{Low}$	$95\%CI_{High}$	$P_{Overall}$	FDR
	Up-regulated in *badR*$^{-}$						
BBG27	hypothetical protein	lp28-2	2.05	1.73	2.44	2.84E-04	5.33E-03
BBF28	hypothetical protein	lp28-1	2.05	1.38	3.03	3.25E-02	1.30E-01
BBL26	hypothetical protein	cp32-8	2.04	1.55	2.69	6.12E-03	4.63E-02
BBR26	hypothetical protein	cp32-4	2.04	1.52	2.73	8.39E-03	5.66E-02
BBE05	hypothetical protein	lp-25	2.02	1.41	2.90	2.40E-02	1.07E-01
BB0519	grpE protein (*grpE*)	chromosome	2.02	1.46	2.81	1.61E-02	8.47E-02
BBP26	hypothetical protein	cp32-1	2.02	1.53	2.67	6.71E-03	4.94E-02
BBN01	hypothetical protein	cp32-9	2.02	1.70	2.40	3.52E-04	6.23E-03
BBE21	hypothetical protein	lp-25	2.01	1.46	2.76	1.41E-02	7.94E-02
BBP04	hypothetical protein	cp32-1	2.01	1.65	2.45	9.54E-04	1.36E-02
	Down-regulated in *badR*$^{-}$						
BBI29	hypothetical protein	lp28-4	−90.58	−128.92	−63.65	3.52E-08	4.93E-06
BBU05	plasmid partition protein, putative	lp21	−51.70	−75.70	−35.31	2.12E-07	1.60E-05
BBI24	hypothetical protein	lp28-4	−40.19	−68.62	−23.54	6.09E-06	2.53E-04
BBI11	hypothetical protein	lp28-4	−35.56	−50.99	−24.80	3.04E-07	2.03E-05
BBI12	hypothetical protein	lp28-4	−30.74	−39.39	−24.00	1.78E-08	4.56E-06
BBI21	hypothetical protein	lp28-4	−27.35	−33.44	−22.36	3.99E-09	1.53E-06
BBI22	conserved hypothetical protein,	lp28-4	−21.83	−27.66	−17.23	2.96E-08	4.74E-06
BBI23	hypothetical protein	lp28-4	−19.25	−25.23	−14.69	1.32E-07	1.35E-05
BBI14	hypothetical protein	lp28-4	−19.18	−25.51	−14.43	2.09E-07	1.60E-05
BBI03	hypothetical protein	lp28-4	−17.79	−29.88	−10.59	3.44E-05	1.15E-03
BBI41	hypothetical protein	lp28-4	−14.57	−16.86	−12.60	1.51E-09	1.16E-06
BBI28	hypothetical protein	lp28-4	−9.99	−16.01	−6.24	9.19E-05	2.24E-03
BBI17	hypothetical protein	lp28-4	−9.68	−13.28	−7.06	4.44E-06	1.95E-04
BBU07	hypothetical protein	lp21	−9.03	−11.11	−7.33	1.72E-07	1.60E-05
BBI20	hypothetical protein	lp28-4	−7.99	−10.45	−6.11	2.42E-06	1.09E-04
BBI16	hypothetical protein	lp28-4	−7.90	−9.97	−6.27	7.45E-07	4.41E-05
BBU04	hypothetical protein	lp21	−7.67	−11.60	−5.07	8.58E-05	2.21E-03
BBI13	hypothetical protein	lp28-4	−6.92	−8.33	−5.74	2.04E-07	1.60E-05

Mol Microbiol. Author manuscript; available in PMC 2016 April 12.

Gene ID	Function (Annotation)	Replicon	$FC_{Overall}$	$95\%CI_{Low}$	$95\%CI_{High}$	$P_{Overall}$	FDR
	Up-regulated in *badR*$^{-}$						
BBI19	hypothetical protein	lp28-4	−6.37	−9.94	−4.09	2.89E-04	5.36E-03
BBI06	pfs protein (pfs)	lp28-4	−6.04	−9.81	−3.72	6.64E-04	1.00E-02
BBI31	hypothetical protein	lp28-4	−5.02	−6.42	−3.92	9.37E-06	3.79E-04
BBI26	multidrug-efflux transporter	lp28-4	−4.59	−7.23	−2.91	1.31E-03	1.67E-02
BBI02	hypothetical protein	lp28-4	−4.35	−5.87	−3.21	9.31E-05	2.24E-03
BB0692	hypothetical protein	chromosome	−3.97	−8.92	−1.77	4.33E-02	1.56E-01
BBU09	hypothetical protein	lp21	−3.57	−6.43	−1.98	1.55E-02	8.29E-02
BB0019	hypothetical protein	chromosome	−3.44	−4.42	−2.68	8.63E-05	2.21E-03
BBI15	hypothetical protein	lp28-4	−3.40	−4.46	−2.59	1.66E-04	3.58E-03
BBA20	hypothetical protein	lp54	−2.87	−5.28	−1.57	3.99E-02	1.47E-01
BB0548	DNA polymerase I (*polA*)	chromosome	−2.84	−4.19	−1.93	4.83E-03	3.99E-02
BBA75	hypothetical protein	lp54	−2.84	−4.78	−1.69	2.17E-02	1.01E-01
BB0310	hypothetical protein	chromosome	−2.82	−5.11	−1.56	3.93E-02	1.46E-01
BBU06	hypothetical protein	lp21	−2.79	−3.37	−2.32	3.65E-05	1.17E-03
BBJ10	hypothetical protein	lp38	−2.78	−4.10	−1.88	5.62E-03	4.48E-02
BBA19	hypothetical protein	lp54	−2.74	−3.85	−1.94	2.92E-03	2.83E-02
BB0077	hypothetical protein	chromosome	−2.73	−3.74	−2.00	1.72E-03	2.08E-02
BBU01	hypothetical protein	lp21	−2.67	−3.67	−1.94	2.16E-03	2.35E-02
BBA21	hypothetical protein	lp54	−2.63	−3.41	−2.03	6.44E-04	9.81E-03
BB0790	hypothetical protein	chromosome	−2.63	−3.88	−1.78	7.65E-03	5.37E-02
BB0210	surface-located membrane protein 1 (*lmp1*)	chromosome	−2.57	−3.50	−1.89	2.21E-03	2.38E-02
BB0828	DNA topoisomerase I (*topA*)	chromosome	−2.57	−3.48	−1.90	2.09E-03	2.33E-02
BB0198	guanosine-3′,5′-bis(di-P) 3′-pyrophosphohydrolase (*RelBbu*)	chromosome	−2.56	−3.14	-2.09	1.37E-04	3.14E-03
BBI01	hypothetical protein	lp28-4	−2.55	−3.57	−1.82	4.18E-03	3.59E-02
BB0200	D-alanine–D-alanine ligase (*ddlA*)	chromosome	−2.52	−3.26	−1.95	8.06E-04	1.17E-02
BBI33	hypothetical protein	lp28-4	−2.49	−3.13	−1.98	4.05E-04	6.85E-03
BBU08	hypothetical protein	lp21	−2.45	−2.99	−2.01	1.70E-04	3.58E-03
BBG31	hypothetical protein	lp28-2	−2.42	−2.83	−2.08	2.69E-05	9.61E-04
BB0197	protoporphyrinogen oxidase, putative	chromosome	−2.38	−3.15	−1.80	2.17E-03	2.35E-02
BB0673	hypothetical protein	chromosome	−2.32	−3.25	−1.66	7.28E-03	5.21E-02

Mol Microbiol. Author manuscript; available in PMC 2016 April 12.

Gene ID	Function (Annotation)	Replicon	$FC_{Overall}$	$95\%CI_{Low}$	$95\%CI_{High}$	$P_{Overall}$	FDR
	Up-regulated in *badR*$^{-}$						
BB0595	hypothetical protein	chromosome	−2.31	−2.82	−1.90	2.70E-04	5.20E-03
BB0251	leucyl-tRNA synthetase (*leuS*)	chromosome	−2.31	−3.04	−1.76	2.31E-03	2.42E-02
BB0012	pseudouridylate synthase I (*hisT*)	chromosome	−2.30	−3.16	−1.67	5.95E-03	4.58E-02
BB0528	aldose reductase, putative	chromosome	−2.29	−3.15	−1.67	5.93E-03	4.58E-02
BB0027	hypothetical protein	chromosome	−2.28	−2.98	−1.75	2.17E-03	2.35E-02
BBU02	hypothetical protein	lp21	−2.27	−3.53	−1.46	3.01E-02	1.25E-01
BBN33	hypothetical protein	cp32-9	−2.24	−3.32	−1.51	1.97E-02	9.49E-02
BBS35	plasmid partition protein, putative	cp32-3	−2.24	−3.34	−1.50	2.18E-02	1.01E-01
BB0184	carbon storage regulator (*csrA*)	chromosome	−2.20	−3.16	−1.54	1.42E-02	7.96E-02
BB0013	hypothetical protein	chromosome	−2.20	−2.82	−1.71	1.90E-03	2.21E-02
BB0363	periplasmic protein	chromosome	−2.19	−2.83	−1.69	2.40E-03	2.44E-02
BB0758	hypothetical protein	chromosome	−2.15	−3.30	−1.40	3.61E-02	1.38E-01
BB0571	uridylate kinase	chromosome	-2.14	-2.83	-1.61	4.89E-03	4.01E-02
BB0782	hypothetical protein	chromosome	−2.10	−2.70	−1.63	3.02E-03	2.90E-02
BBB11	hypothetical protein	cp26	−2.09	−2.62	−1.67	1.48E-03	1.84E-02
BB0768	pyridoxal kinase (*pdxK*)	chromosome	−2.09	−2.60	−1.68	1.22E-03	1.63E-02
BBB01	hypothetical protein	cp26	−2.08	−2.76	−1.58	5.61E-03	4.48E-02
BB0754	ABC transporter, ATP-binding protein	chromosome	−2.08	−2.87	−1.51	1.19E-02	7.11E-02
BBH27	hypothetical protein	lp28-3	−2.08	−2.96	−1.45	1.96E-02	9.49E-02
BB0305	hypothetical protein	chromosome	−2.08	−3.16	−1.36	3.98E-02	1.47E-01
BBB29	PTS system, maltose and glucose-specific IIABC component (*malX*)	cp26	−2.05	−2.63	−1.60	3.15E-03	2.97E-02
BBA42	hypothetical protein	lp54	−2.05	−3.17	−1.33	4.83E-02	1.69E-01
BB0080	ABC transporter, ATP-binding protein	chromosome	−2.05	−2.82	−1.49	1.29E-02	7.48E-02
BB0587	methionyl-tRNA synthetase	chromosome	−2.05	−2.86	−1.47	1.58E-02	8.41E-02
BB0078	hypothetical protein	chromosome	−2.04	−3.12	−1.33	4.54E-02	1.62E-01
BB0749	hypothetical protein	chromosome	−2.03	−2.73	−1.52	8.88E-03	5.91E-02
BB0009	hypothetical protein	chromosome	−2.03	−3.08	−1.34	4.31E-02	1.56E-01
BB0308	hypothetical protein	chromosome	−2.02	−2.89	−1.42	2.29E-02	1.03E-01
BB0249	phosphatidyltransferase	chromosome	−2.02	−2.56	−1.60	2.47E-03	2.49E-02
BBS36	hypothetical protein	cp32-3	−2.02	−2.62	−1.56	4.61E-03	3.83E-02

Mol Microbiol. Author manuscript; available in PMC 2016 April 12.

Gene ID	Function (Annotation)	Replicon	$FC_{Overall}$	$95\%CI_{Low}$	$95\%CI_{High}$	$P_{Overall}$	FDR
	Up-regulated in *badR*$^{-}$						
BB0838	hypothetical protein	chromosome	−2.02	−3.09	−1.32	4.85E-02	1.69E-01

[*] Function (Annotations) are based on JCVI/CMR *B. burgdorferi* strain B31-and in (Fraser *et al.*, 1997).

[†] $FC_{Overall}$= fold changes are between B31-A3 (WT) and *badR*$^{-}$ and derived by pooling both independent microarrays.

[‡] $P_{Overall}$= P value derived by pooling both independent microarrays.

[§] Genes ≥2 fold differences in expression and $P_{Overall}$ ≤0.05 are reported.

[¶] 95%CILow-High =95% confidence intervals indicating range of fold change expression.

[//] FDR = adjusted Benjamini-Hochberg False Discovery Rates are all statistically significant (≤0.2).

[**] Genes validated by qRT-PCR and/or western blotting are bolded.

Mol Microbiol. Author manuscript; available in PMC 2016 April 12.

Table 2

Quantitative RT-PCR of select genes.

Gene ID	Function (Annotation)	Array	qRT-PCR
BB0771	RNA polymerase sigma factor (*rpoS*)	2.1	26.06
	RNA polymerase sigma factor (*rpoS*) – long transcript	N/A	3.75
BBB19	outer surface protein C (*ospC*)	75.2	55.38
BBA24	decorin binding protein A (*dbpA*)	7.7	30.91
BBA34	oligopeptide ABC transporter, periplasmic oligopeptide-binding protein (*oppAV*)	7.8	211.37
BBB05	PTS system, chitobiose-specific IIA component (*chbC*)	24.1	54.21
BB0240	glycerol uptake facilitator (*glpF*)	1.8	7.04
BBI42	hypothetical protein	5.0	7.07
BBA07	chpAI protein, putative	17.7	362.04
BBP27	rev protein	12.5	35.59
BBP28	lipoprotein	10.0	16.95
BBB29	PTS system, maltose and glucose-specific IIABC component (*malX*)	−2.1	−3.07
BBI16	hypothetical protein	−7.9	Undetectable
BB0019	hypothetical protein	−3.4	−1.44
BB0198	guanosine-3′,5′-bis(di-P) 3′-pyrophosphohydrolase (Rel_{Bbu})	−2.6	−1.19
BBU05	plasmid partition protein, putative	−51.7	Undetectable

*Function (Annotations) are based on JCVI/CMR *B. burgdorferi* strain B31-and in (Fraser *et al.*, 1997).

†Exception of *rpoS* long transcript; qRT-PCR primers were used (Table S3) to amplify only the long *rpoS* transcript variant.

‡Values expressed as a ratio of expression for the gene in B31-A3 WT relative to *badR*⁻ and derived by pooling both independent microarrays.

Table 3

Plasmids and strains used in this study.

Plasmids	Description	Source or reference
pCR®2.1-TOPO	PCR cloning vector	Invitrogen
pET23a	Expression vector with a C-terminal 6-His tag	Novagen
pMALc2x	Protein expression vector	NEB
pCLM11	BB0693 cloned into pET23a	This study
pCLM25	BB0693 cloned into pMALc2x	This study
pCLM40	BB0693NoHTH cloned into pMALc2x	This study
pCLM55	BB0693NoIBD cloned into pMALc2x	This study
pCLM67	BB0693H243A cloned into pMALc2x	This study
pCLM66	BB0693C254A/C257A cloned into pMALc2x	This study
pCLM65	BB0693N253A/P255A cloned into pMALc2x	This study
pMP2	BB0151 cloned into pET23a	This study
pMP3	BB0152 cloned into pET23a	This study
pCLM22	BB0645 cloned into pET23a	This study
pTS2	BBB05 cloned into pET23a	This study
pBVSR2713	BB0831 cloned into pET23a	This study
pMP4	BB0545 cloned into pET23a	This study
pCLM26	BB0055 cloned into pET23a	This study
pBVSR3212	BB0694 cloned into pET23a	This study
pCLM12	upstream (732988–734094) and downstream (735259–736264) flanking Str^r cassette in pCR2.1 for BB0693 deletion 733108–735289 upstream and BB0693 and 735290–736288 downstream	This study
pCLM24	flanking Gent^r cassette for BB0693 cis complementation	This study
***B. burgdorferi* strains**	**Description**	**Source or reference**
A3	B31, low passage parental infectious isolate (WT)	(Elias *et. al* 2002)
badR$^-$	B31 isolate, *badR* (BB0693)deficient, Str^r	This study
badR2$^-$	B31 isolate, *badR* (BB0693) deficient, Gent^r	This study

Str^r, streptomycin resistance; Gent^r, kanamycin resistance.

Table 4

Mammalian infectivity analysis of *badR*-deficient strains.

No. of cultures positive /total No.									No. of mice positive/total No. of mice
Mouse strain	**Strain**	**Skin**	**Lymph**	**Spleen**	**Bladder**	**Heart**	**Joint**	**All sites**	
C3H/HeN	A3	5/5	5/5	5/5	5/5	5/5	5/5	30/30	5/5
	badR1⁻	0/5	0/5	0/5	0/5	0/5	0/5	0/30	0/5
	badR2⁻	0/5	0/5	0/5	0/5	0/5	0/5	0/30	0/5
BALB/c	A3	3/3	3/3	3/3	3/3	3/3	3/3	18/18	3/3
	badR1⁻	0/3	0/3	0/3	0/3	0/3	0/3	0/18	0/3
	badR2⁻	0/3	0/3	0/3	0/3	0/3	0/3	0/18	0/3
SCID	A3	3/3	3/3	3/3	3/3	3/3	3/3	18/18	3/3
	badR1⁻	0/3	0/3	0/3	0/3	0/3	0/3	0/18	0/3
	badR2⁻	0/3	0/3	0/3	0/3	0/3	0/3	0/18	0/3